

University of Windsor

## Scholarship at UWindor

---

Electronic Theses and Dissertations

Theses, Dissertations, and Major Papers

---

1-1-1989

### Restoration of motion blurred images.

Amol James Kekre  
*University of Windsor*

Follow this and additional works at: <https://scholar.uwindsor.ca/etd>

---

#### Recommended Citation

Kekre, Amol James, "Restoration of motion blurred images." (1989). *Electronic Theses and Dissertations*. 6838.

<https://scholar.uwindsor.ca/etd/6838>

This online database contains the full-text of PhD dissertations and Masters' theses of University of Windsor students from 1954 forward. These documents are made available for personal study and research purposes only, in accordance with the Canadian Copyright Act and the Creative Commons license—CC BY-NC-ND (Attribution, Non-Commercial, No Derivative Works). Under this license, works must always be attributed to the copyright holder (original author), cannot be used for any commercial purposes, and may not be altered. Any other use would require the permission of the copyright holder. Students may inquire about withdrawing their dissertation and/or thesis from this database. For additional inquiries, please contact the repository administrator via email ([scholarship@uwindsor.ca](mailto:scholarship@uwindsor.ca)) or by telephone at 519-253-3000ext. 3208.

**RESTORATION OF MOTION BLURRED IMAGES**

by

**Amol James H Kekre**

**A Thesis submitted to the  
Faculty of Graduate Studies and Research  
through the Department of Electrical Engineering  
in Partial Fulfillment of the requirements  
for the Degree of Master of Applied Science  
at the University of Windsor**

**Windsor, Ontario, Canada**

**1989**

UMI Number: EC54829

### INFORMATION TO USERS

The quality of this reproduction is dependent upon the quality of the copy submitted. Broken or indistinct print, colored or poor quality illustrations and photographs, print bleed-through, substandard margins, and improper alignment can adversely affect reproduction.

In the unlikely event that the author did not send a complete manuscript and there are missing pages, these will be noted. Also, if unauthorized copyright material had to be removed, a note will indicate the deletion.

**UMI<sup>®</sup>**

---

UMI Microform EC54829  
Copyright 2010 by ProQuest LLC  
All rights reserved. This microform edition is protected against  
unauthorized copying under Title 17, United States Code.

---

ProQuest LLC  
789 East Eisenhower Parkway  
P.O. Box 1346  
Ann Arbor, MI 48106-1346

## ABSTRACT

Image restoration is an important part of any image understanding system. One of the most common source of degradation is due to motion blur and focus blur. Valuable information contained in blurred images can be extracted only if these blurs are successfully removed.

This thesis deals with the problem of restoring images blurred by linear spatially invariant rigid body motion blur. In this thesis first a review of important techniques for restoration of blurred images is given. It is shown that the majority of the restoration techniques require a priori knowledge of certain parameters in their degradation model to yield successful results. Therefore the robustness of any algorithm depends on its success under the wrong estimate of these parameters. This thesis discusses various methods to extract the value of the blur parameters in three domains, namely, spatial, frequency and cepstral domain.

In this thesis an algorithm based on a reverse mapping technique is developed to restore motion blurred images. Also presented are details of issues involved in the reverse mapping algorithm along with the advantages and

disadvantages of the technique. The proposed algorithm is then used on a variety of motion blurred images to demonstrate its usefulness and robustness.

## ACKNOWLEDGEMENTS

I sincerely acknowledge my co-supervisor, Prof M. Ahmadi for his guidance and help in this research. I would also like to thankfully acknowledge, my co-supervisor, Prof M. Shridhar for his kind guidance and assistance. I would like to extend my gratitude to the committee members, Prof J.J. Soltis and Prof R. Yazdi for their valuable suggestions during the progress of this research.

## CONTENTS

Abstract .....	ii
Acknowledgements .....	iv
<u>Chapter 1 - Introduction</u>	
Problem Definition .....	2
Sources and Types of Motion Blurs .....	7
The Impulse Matrix .....	13
Cepstral Domain .....	18
A Survey of Image Restoration Techniques and Applications	20
<u>Chapter 2 - Image Restoration Techniques</u>	
Introduction .....	29
Definitions .....	29
Constraints .....	30
Projections Onto Convex Sets ( POCS ) .....	30
Feasible Set .....	32
Convergence Rate, Path and Criteria .....	33
Eigenvalues and the Lost Information .....	34
Continuity or Smoothness .....	35
Dynamic range .....	35
Residual Outliers .....	36
A Dynamic System Model .....	36
Generation of Information from Background Pixels .....	41
The Landweber Iteration .....	41

Some of the Important Image Restoration Techniques .....	43
Minimization of the Mean Squared Error ( MSE ) .....	44
Conditional Expectation .....	45
Singular Value Decomposition ( SVD ) .....	46
Inverse Filtering .....	47
Data Extraction Techniques ( Blur parameter ) .....	49
Frequency Domain Approach .....	49
Cepstrum Domain Approach .....	50
Spatial Domain Approach .....	50
Multiple Degradations .....	51
Double Convolution Model ( Cascading of blurs ) .....	52
Bilinear Model .....	53
Conclusions .....	54

### Chapter 3 - Restoration by Reverse Mapping

Introduction .....	56
Rigid Body Uniform Linear Motion Blur .....	57
General Degradation .....	71
Implementation Issues .....	75
Parallel Hardware Implementation .....	75
Noise Sensitivity .....	77
Blur Parameter Estimation .....	77
Constraints .....	78
Kalman Filtering .....	79
Advantages and Drawbacks of Reverse Mapping Algorithm ...	79
Conclusions .....	81
Results .....	82



Chapter 4 - Summary and Conclusions

..... 106

Appendix A ..... 109

Appendix B ..... 113

Appendix C ..... 115

Appendix D ..... 117

Appendix E ..... 119

Appendix F ..... 120

Appendix G ..... 122

Bibliography ..... 123

Vita Auctoris ..... 129

## FIGURES

1.	The Motion Blur Model .....	4
2.	A Computer Simulated Motion Blur .....	5
3.	Spatial Domain Discretization Formats .....	9
4.	Hurter-Driffield Curve .....	10
5.	An Image Forming System .....	12
6.	The Dynamical Model ( State-Space ) .....	40
7.	Parallel Hardware Implementation .....	76
8.	Set of Images of a Chessboard .....	85
9.	Set of Images of a Piston .....	88
10.	Set of Images of Toys .....	91
11.	Set of Images of a Dollar Bill .....	94
12.	Noise Performance on a Dollar Bill .....	97
13.	Robber's Images .....	100
14.	Blur Parameter Sensitivity .....	102
15.	Set of Images of the face of a lady .....	104

## CHAPTER I

### INTRODUCTION

In recent decades with the advent of high resolution cameras and digital computers, the use of visual information has become important and possible in many scientific applications. The speed and accuracy of a digital computer makes it possible to interpret this data reliably. The decision making can be done by a digital computer or by a human. This visual information is in the form of two dimensional digital images. Some examples of the application of digital imagery are crop prediction, satellite tracking, robotics, medicine etc.

This use of digital images, in a decision making process has made it necessary to acquire an ability to accurately identify objects in the images. Due to various factors in nature, these images are often blurred making identification of objects and hence interpretation difficult. Scientists have thus given importance to image restoration as an integral part of visual interpretation. Blurs are a very prominent class of image degradations. This thesis deals with restoring images blurred by relative motion between the object and the camera.

In the next section, the problem of restoring images blurred by motion is defined. The sources and different types of motion blurs are discussed in Section 1.2. The impulse matrix is studied in Section 1.3. The cepstrum domain is studied in Section 1.4. Finally a brief literature survey of image restoration techniques is done in Section 1.5.

### 1.1 Problem Definition

The problem tackled in this thesis is to obtain the original image, once the image degraded due to motion is given. This degradation can be treated as a filter for nearly all the motion blurs. As shown in Figure 1, the degraded image  $g(x,y)$  is assumed to have been obtained, by passing the original image  $f(x,y)$  through the motion blur filter  $H$ , in the presense of the additive noise  $n(x,y)$ . The degraded image is restored by implementing techniques that are known to succeed on such filters. This can also be stated as determining the mathematical operation to be performed on the degraded image to get the original image. Figure 2 shows an original image of a chess board with the corresponding degraded image. This was obtained by passing the original image through a computer simulated motion blur filter, in the absence of noise.

The characteristics of this filter depend upon the type

of motion blur. The sources and types of motion blur are discussed in the next section. This thesis studies linear spatially invariant rigid body motion blur. As shown in Figure 1, noise is assumed to be additive. In this case the filter is best denoted by a convolution model as in Equation ( 1-1 ). This gives the mathematical definition of the motion blur.

The convolution model is one of the most widely used for motion blurs. Equation ( 1-1 ) gives the continuous convolution model for a two dimensional motion blur as in [1] - [17], [25], [31], [33] - [36].

$$g(x,y) = \int_{-\infty}^{\infty} \int_{-\infty}^{\infty} h(\alpha,\beta) f(x-\alpha,y-\beta) d\alpha d\beta + n(x,y) \quad \dots\dots\dots ( 1-1 )$$

Where :

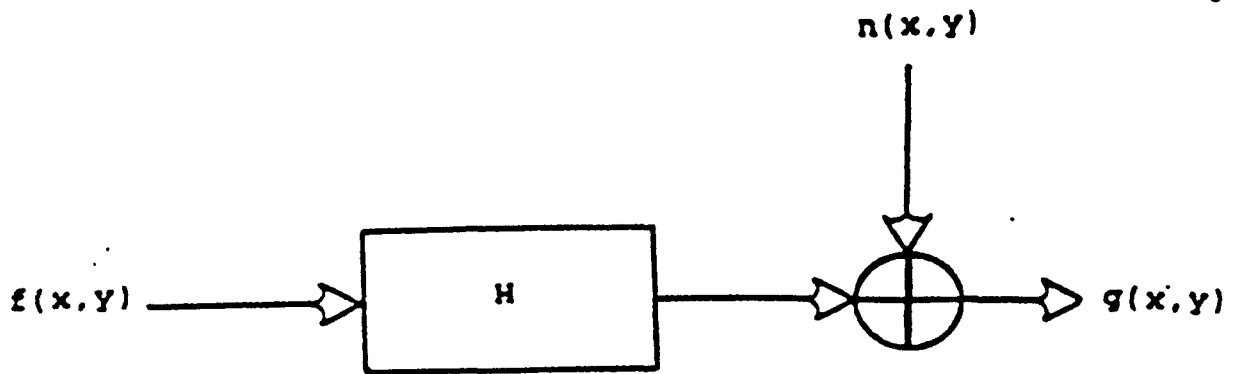
$g(x,y)$  - the degraded image.

$f(x,y)$  - the original image.

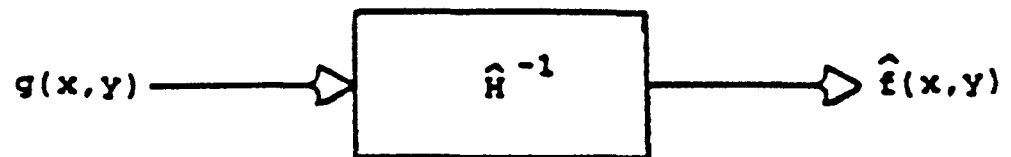
$h(\alpha,\beta)$  - the impulse response of the degradation filter, also called the point spread function ( PSF ) of the filter.

$n(x,y)$  - the additive noise.

The model given by Equation ( 1-2 ) is a discrete equivalent for the digital computer as in [1]- [7], [11], [14], [17], [34] - [36]. Since the impulse response for motion blurs is finite in nature, the limits of integration



(a) The Blur Model



(b) The Restoration Model

Figure 1. The Motion Blur Model.

Where :

$g(x,y)$  is the degraded image.

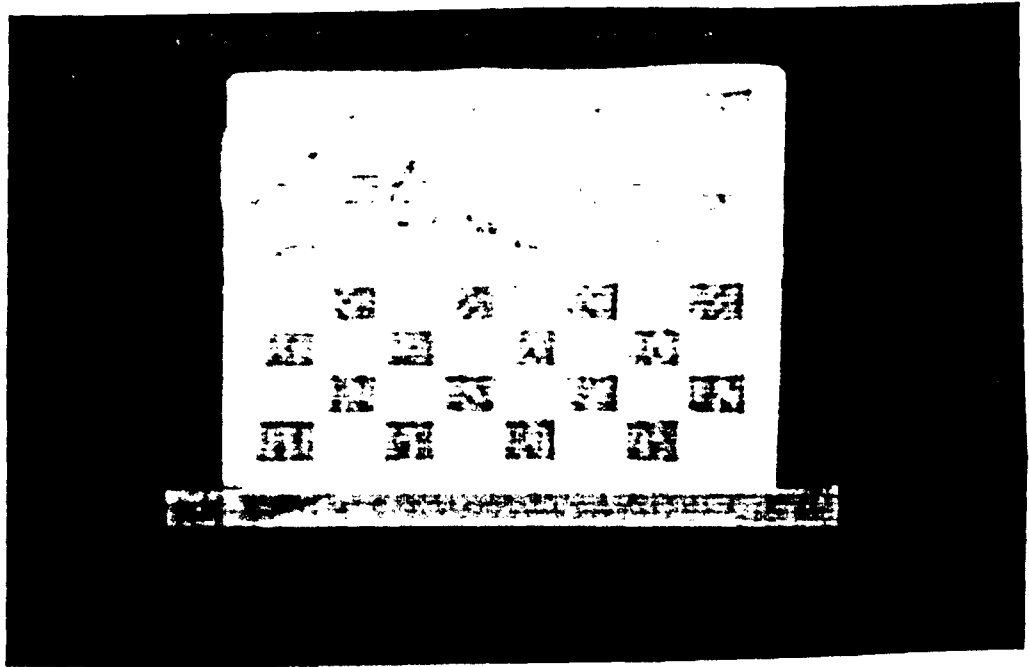
$f(x,y)$  is the original image.

$\hat{f}(x,y)$  is the estimate of the original image.

$H$  is the Motion Blur filter.

$\hat{H}^{-1}$  is the Restoration filter.

$n(x,y)$  is assumed to be zero.



(a)



(b)

**Figure 2. A Computer Simulated Motion Blur Image.**

(a) The original image.

(b) The blurred image.

are modified to  $\pm M$ .

$$g(x,y) = \sum_{i=-M}^M \sum_{j=-M}^M h(i,j) f(x-i,y-j) + n(x,y) \quad \dots\dots\dots (1-2)$$

In Equation (1-2) all the notations are discrete equivalents of Equation (1-1). These discrete samples are called pixels.

The digital convolution is implemented on computers in the form of matrices as in [2] - [10], [13], [14], [18]. The discrete samples are converted into matrix formats as follows.

$$[g] = [h][f] + [n] \quad \dots\dots\dots (1-3)$$

Where :

[g] - is a matrix of order  $N \times N$  representing the degraded signal.

[f] - is a matrix of order  $M \times N$  representing the original signal.

[h] - is the impulse matrix of the order  $N \times M$ .

[n] - is a matrix of order  $N \times N$  representing noise.

Here  $M > N$ , i.e., a loss of information has taken place.

This also means that the impulse matrix is singular. Thus image restoration can be defined as the extraction of this lost information.



## 1.2 Sources and Types of Motion Blurs

An optical system is defined as a system consisting of the camera tracking the object(s) with a transparent medium in between them. Images get degraded due to imperfections in any part of this optical system.

Blurs are one of the degradations resulting from an imperfect camera tracking ( motion and focus blurs ). Other sources of degradations are grain noise or over/under exposure of film. The image degradations due to imperfect objects include sun photography, sky and star's images, nuclear reactor core, snow gaze, etc. Image degradations due to imperfect medium are underwater photography, fog, atmospheric turbulence, etc.

Camera errors mostly give rise to linear image degradations. Image degradations due to object errors are both linear and non linear. Image degradations due to the medium are mostly non linear.

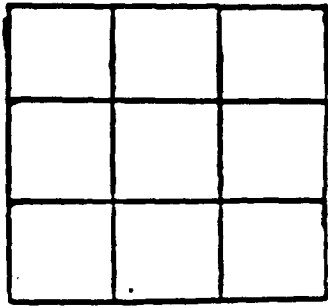
Motion blurs are caused by a relative motion between an object(s) being photographed and the camera. There is a different degradation for each type of relative motion. The main types of motions are translation along the plane perpendicular to the optical axis, translation parallel to the optical axis ( assumed to be the z axis ), rotation

about any random axis and any combination of the above. Motion blur is classified into different types based on the source of the motion blur. In this section the types related to this thesis are discussed.

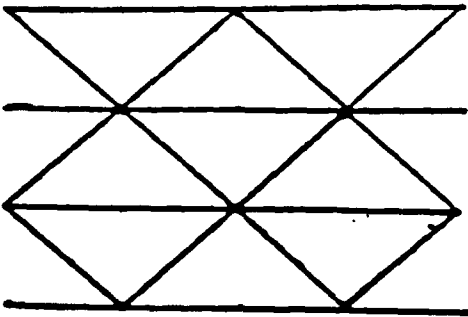
Motion blurs can be classified as spatially variant and spatially invariant blurs. This classification depends upon the co-ordinate system used. It also depends upon the spatial discretization formats which are rectangular, triangular and hexagonal format as shown in Figure 3. This thesis uses only the cartesian co-ordinate system ( square discretization ). The orthogonality of this system has made it an universally accepted format for image discretization. Images used in this thesis are in the form of two dimensional data matrix with each location being a pixel element.

Motion blurs are also classified as linear blurs or non linear blurs. A majority of motion blurs are linear transformations of the original image pixels into the degraded image pixels. The exceptions take place due to the non linearities of the film response and a non planar structure of the object.

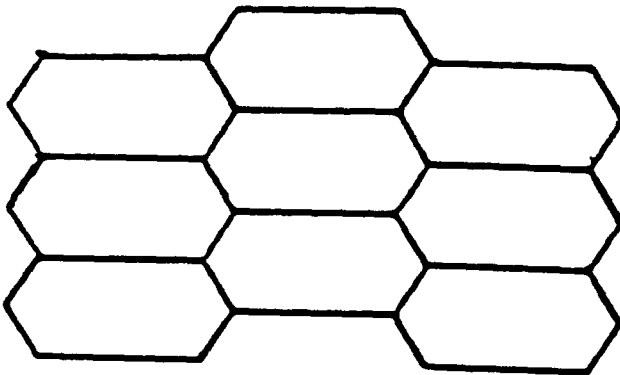
The film response of a typical film is given by the Hurter-Driffield curve given in Figure 4. The Hurter-Driffield curve plots the film response ( logarithm of the



(a) Rectangular Format.



(b) Triangular Format.



(c) Hexagonal Format.

Figure 3. Spatial Domain Discretization Formats.

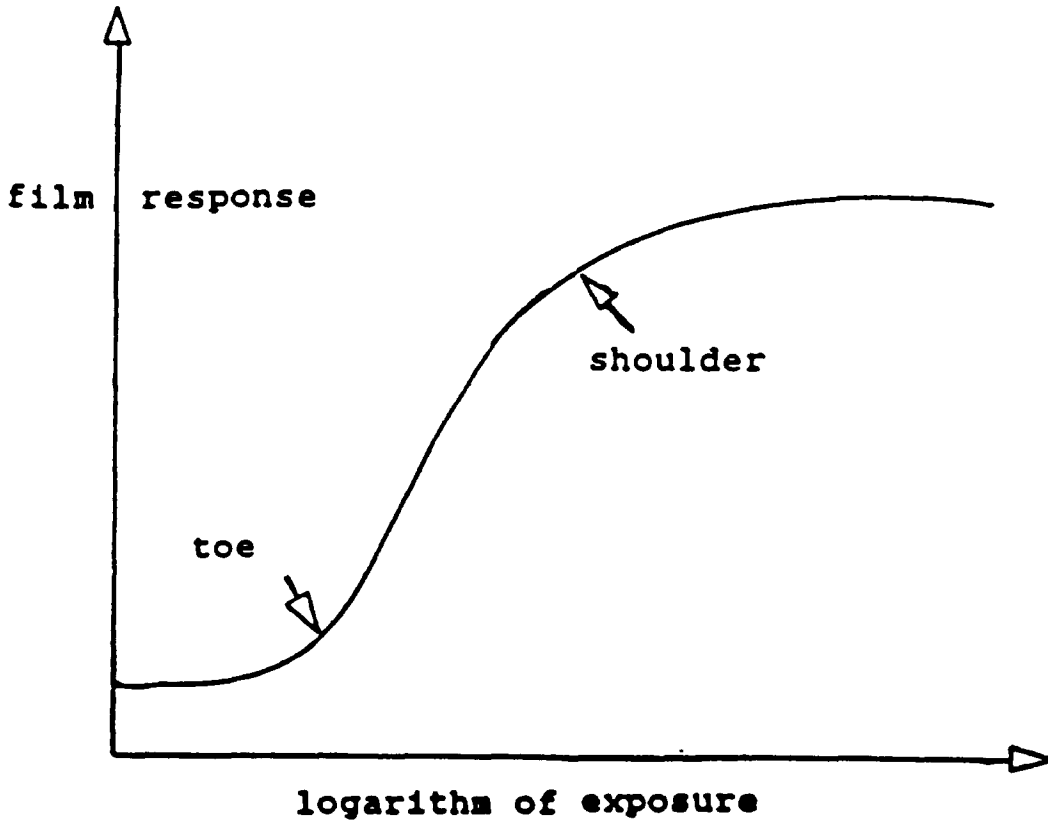


Figure 4. Hurter-Drifffield Curve.

ratio of the incident light intensity to the transmitted light intensity ) and the logarithm of the exposure ( light energy per unit area ). The upper and the lower regions of the curve are called the shoulder and the toe respectively. The linear region is in between the toe and the shoulder. The slope of the linear region is called the gamma of the curve. The film response is linear only in the gamma region, as stated in [1] and [34].

Non linearities due to the non planar structure of the object are best defined by irradiance  $R$ , i.e., the light energy flux incident on an infinitesimal surface element  $dA$ , as follows. Ballard et al. [1] have proved that this is a source of non linearity due to the variations of the off axis angle  $\Omega$  ( see Figure 5 ) of the object.

$$R = K \cos^4(\Omega) \dots\dots\dots ( 1-4 )$$

Where

$K$  : is a constant depending upon the focal length, the surface area of the lens and the distance between the lens and the object.

$\Omega$  : is the off axis angle as in Figure 5 .

$R$  : is the irradiance, i.e., the light energy flux incident on an infinitesimal surface element  $dA$ .

In this thesis the off axis angle  $\Omega$  is assumed to be constant. This is based on the assumption that the object is planar and the camera-object distance is large compared

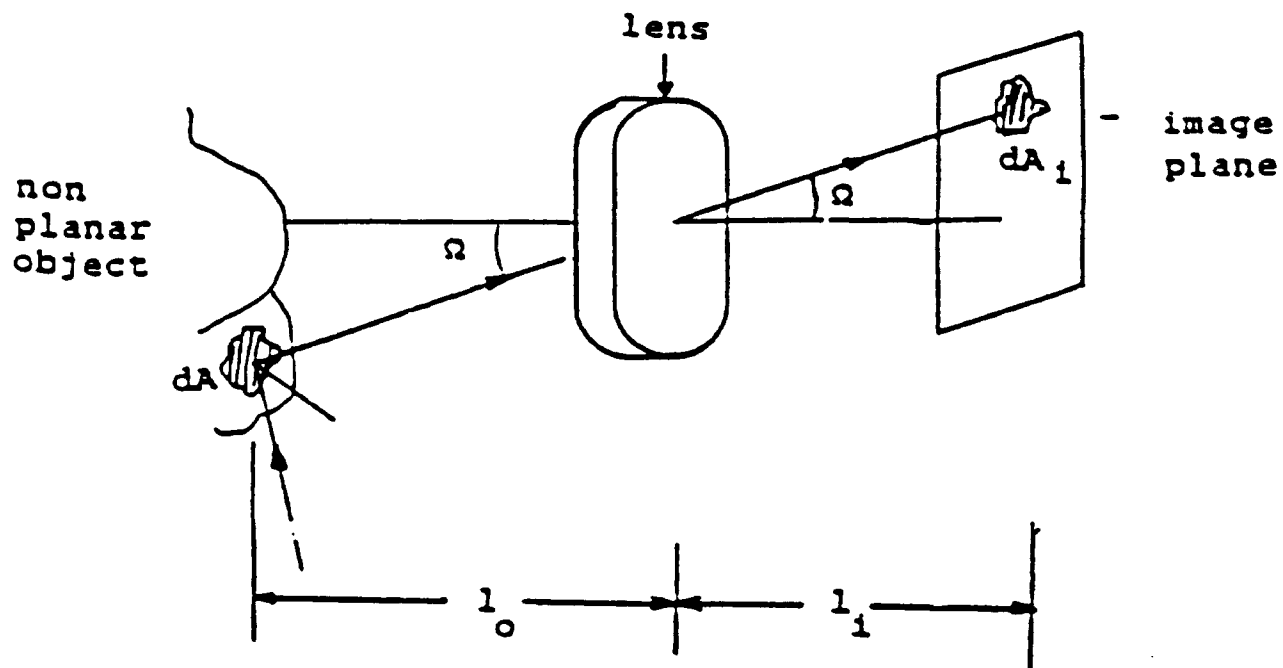


Figure 5. An Image Forming System.

to the size of the object.

Motion blur can also be one involving a rigid body even if there are multiple objects. Silverman et al. [11], [12], [13] defined rigid body motion blur as, "if the motion is such that the object always shows the same face towards the imaging system and the object image distance remains constant, then the object appears at each instant as a translated or rotated version of what is termed as the object plane. Thus the motion may be interpreted as a relative motion and translation of two constant distance parallel planes - the image plane associated with the imaging system and the object plane associated with the object. The intensity at each point of recorded image ( pixel ) is a combination of intensities of the several object plane points passing beneath that point during the exposure".

### 1.3 The Impulse Matrix

The problem of deblurring using a digital computer involves the implementation of blur filter as a matrix, called the impulse matrix (  $[ h ]$  in Equation ( 1-3 ) ). In this section the impulse matrix for a linear spatially invariant rigid body motion blur is studied.

The impulse matrix for any linear motion blur filter can

always be expressed in the form of a Toeplitz matrix as in [1], [2], [11], [25], [34]. But for a general linear motion blur, Toeplitz matrix has a very high order [1] and [34]. In the case of a rigid body motion blur the order of the impulse matrix can be significantly reduced.

The impulse matrix denotes the matrix equivalent of the blur filter in the simplest form possible. It is the most important information involved in the deblurring the motion blurred image. Silverman et al. [11] - [13], Sondhi [2], Trussell et al. [14] - [16], Harris [3] - [4] and Horner [5] - [6] have proved that in the case of a linear and spatially invariant rigid body motion blur, the impulse matrix is always singular. This means that a loss of information has taken place, as shown in [2], [14] - [18].

Loss of information can also be visualized as a lack of sufficient equations to solve for original image. Equation ( 1-3 ) shows that there are  $N^2$  equations to solve for  $N \times M$  variables (  $M > N$  ). In certain other cases of motion blur like  $z$  directional motion, the original set may consists of  $M_1 \times M_2$  but the loss of information still takes place in all these cases of motion blur, as proved in [2], [11], [12], [16].

The ease with which the lost information can be extracted depends upon the set of equations provided by



Equation ( 1-3 ). This implies that the most important factors in deblurring are the impulse matrix and the presense of noise.

Depending on the type of motion blur, the impulse matrix is classified as spatially invariant point spread function ( SIPSF ) or spatially variant point spread function ( SVPSF ). The impulse matrix is also defined as a many-to-one mapping function between the original image and degraded image. The restoration is then viewed as a reverse mapping. This problem has infinite solutions. In the later chapters a method is developed to select the best possible solution.

Without loss of generality, in this section it is assumed that the direction of motion is along the x direction. The degraded and the original signal are therefore denoted by the corresponding one dimensional vector. This is done because the motion blur is independant of the direction perpendicular to the motion ( i.e., the y axis ).

$$\begin{aligned} 0 &\leq g(x) \leq g_{\max} & x \in [1, N] \\ 0 &\leq f(x) \leq f_{\max} & x \in [1, M] \end{aligned} \quad \dots\dots\dots ( 1-5 )$$

Where

$$g_{\max} = f_{\max} = 255.$$

Since  $g_{\max}$  and  $f_{\max}$  same, we have Equation ( 1-6 ).

$$\sum_{i=-M}^M \sum_{j=-M}^M h(i,j) = 1 \quad \dots\dots\dots ( 1-6 )$$

Equation ( 1-6 ) could also be proved using the law of conservation of energy as in [2], [18]. In the case of rigid body uniform linear motion, the lower limit on the summation in Equation ( 1-6 ) can be put to zero.

The amount of lost information is decided by the type of degradation i.e., the impulse matrix. But it is also expressed in the form of the blur parameter.

Sondhi [2] defined the blur parameter as, " a variable(s) which characterises any blurring". Tekalp et al. [25] defined it as, " the parameter(s) which determines the PSF so as to completely identify it". Broida et al. [24] defined it as, " the parameter(s) which defines the model used to describe the degradation filter".

For motion blur the blur parameter is the distance moved 'd', while for focus blur it is the defocus radius 'r'. Trussell et al. [18] established an empirical relation between the blur parameter and the eigenvalues of the impulse matrix and their effect on restoration.

The impulse response of the blur filter to any linear motion, is the response of the filter to a unit impulse in the direction of motion. The impulse response for uniform linear motion is given below. The impulse matrix is the impulse response in a matrix notation.

Let  $\delta(\theta)$  be the unit impulse in the direction  $\theta$ . If  $d$  is the total distance moved then the impulse response is as follows.

$$h(x,y) = \begin{cases} \{ 1/v(\theta) \} \delta(\theta) & 0 \leq x \leq d \cos(\theta) \\ & 0 \leq y \leq d \sin(\theta) \\ 0 & \text{else} \dots\dots\dots (1-7) \end{cases}$$

Where

$v(\theta)$  : The constant speed in direction.

The frequency response of this filter is

$$\begin{aligned} H(u,v) &= \sin(\pi df) / (\pi df) \\ &= \text{sinc}(\pi df) \dots\dots\dots (1-8) \end{aligned}$$

Where

$$f = u \cos(\theta) + v \sin(\theta)$$

$u, v$  : are the frequency co-ordinates.

The loci of the zeros of the impulse response is perpendicular to the direction of motion. Equation (1-9) shows that they lie a distance  $(1/d)$  apart.

$$\text{Sinc}(\pi df) = 0$$

$$\pi df = n \pi \quad ( n \text{ is an integer } )$$

ie the loci is,

$$\text{frequency } f = n/d$$

$$= n (1/d) \quad \dots\dots\dots ( 1-9 )$$

A special case is x direction motion. The impulse matrix is x direction linear and spatially invariant rigid body uniform motion blur is as follows.

$$h(x,y) = \begin{cases} 1/d & 0 \leq x \leq d. \\ & y = 0 \\ 0 & \text{else } \dots\dots\dots ( 1-10 ) \end{cases}$$

1.4 Cepstral Domain

Cepstrum domain processing is used for deconvolution of two signals [22]. There are three types of cepstrums, namely, complex cepstrum, power cepstrum and phase cepstrum. The units of a parameter in the cepstral domain are the units of that parameter in the time domain. To avoid confusion Bogert et al. [22], [31] and [35] proposed the following paraphrases.

Time domain units	Cepstrum domain units
frequency .....	quefrency
spectrum .....	cepstrum
phase .....	saphe

magnitude ..... gamnitude  
 filtering ..... liftering  
 harmonic ..... rahmonic  
 period ..... repiod ..... ( 1-11 )

The power cepstrum was first defined by Bogert et al. Equation ( 1-12 ) is a very useful tool in data extraction.

$$g_{pc}(nT) = \text{IFFT}(\ln|(u,v)|) \quad \dots\dots\dots ( 1-12 )$$

Where

- $g_{pc}$  : is the power cepstrum of the degraded signal.
- $T$  : the sampling time period.
- $\ln$  : stands for natural logarithm.
- $n$  : denotes the  $n$  th sample.

Complex cepstrum as a tool for deblurring was first introduced by Oppenheim [31], [35] and [29]. He used complex cepstrum for signal recovery.

$$g_{cc}(nT) = \text{IFFT}(\text{cln}(G(u,v))) \quad \dots\dots\dots ( 1-13 )$$

Where

- $g_{cc}$  : is the complex cepstrum of the degraded signal.
- $\text{cln}$  : stands for complex natural logarithm.

From Equations ( 1-13 ) and ( 1-2 ), in the absence of noise,

$$g_{cc}(nT) = f_{cc}(nT) + h_{cc}(nT) \quad \dots\dots\dots ( 1-14 )$$

Where

- $g_{cc}$  : is the complex cepstrum of the degraded signal.

$f_{cc}$  : is the complex cepstrum of the original signal.

$h_{cc}$  : is the complex cepstrum of the impulse matrix.

Ahmadi et al. [27] have shown that the properties of the cepstrum are related to the stability of the impulse response ( of a digital recursive filter ). Hence this information is also useful in the dynamical system approach where the stability of the filter is an important information regarding the feasibility of any restoration.

Complex logarithm is a multivalued function. This sometimes gives rise to unwrapping errors. Unwrapping errors can be avoided by integrating the phase derivative or sequential unwrapping as shown in [22].

The main drawback of the cepstral domain processing is that it is more sensitive to noise than both the other domains. However, cepstral domain processing is a very useful tool for data extraction ( i.e., blur parameter estimation ).

### 1.5 A Survey of Image Restoration Techniques and Applications

Image restoration techniques are algorithms used to extract the original image from the degraded one. There are several image restoration techniques developed in the last two decades. These differ in terms of the domains in which

image restoration is carried out as well as the approaches used, for example, deterministic or stochastic, adaptive or static, iterative or non iterative, etc.

Image restoration techniques are classified as iterative and non iterative. Iterative techniques reach the final solution in steps, using the result of the previous step(s) as a guide for further improvement. They exit when no further improvement is possible. Non iterative techniques consist of a single step approach. Iterative image restoration techniques try to minimize some error criteria or to maximize some performance criteria. Iterative image restoration techniques take more computational time, and also have a much greater control over the restoration ( and thus the final solution ). In this thesis iterative image restoration techniques are considered.

In any image restoration application, two main problems have to be solved. The first step is to obtain data regarding the impulse matrix ( or the blur parameter). This falls under the class of data extraction techniques which are specifically designed just to find the impulse matrix i.e., the blur parameter. This is a very important part of blur removal because the performance of any image restoration technique is very sensitive to an accurate knowledge of the blur parameter. The second step is to implement the image restoration technique. In this chapter a

brief survey of image restoration techniques is presented.

The first successful mathematical modelling of motion blur as a filter was developed by Marechal et al. ( see [2] ). Motion blur as a filter operating on the original image is now an established blur model.

Oppenheim [29] - [31] and Schafer [35] evaluated and developed models in non linear filtering of blurs using a combination of homomorphic filtering and inverse filtering. Oppenheim proposed a theory of combining linear prediction with homomorphic filtering calling it as homomorphic Prediction [29]. Homomorphic signal processing, a non linear technique based on linear filtering operations on the complex cepstrum of the blurred signal was introduced by Oppenheim et al. [31].

Cannon used blind deconvolution [31] as an inverse of convolution filter models in the cepstrum domain. This meant averaging in the cepstrum domain to get an approximate idea of the blur parameter, thereby improving the deblur filter performance.

Sondhi [2] reviewed spatial domain image restoration techniques for linear motion blurs. Sondhi [2] established the accuracy of the assumptions of linear and spatially invariant models of a great variety of configurations of



practical interest.

The technique of minimizing least square errors between the blurred signal and an estimate of it, was shown to have a very good performance in blur restoration by Harris [3] - [4], Horner [5] - [6] and by Helstrom [7]. Helstrom [7] pioneered the technique of using the conditional expectation of the original signal in solving for the information lost. Harris and Horner [3] - [4] developed a varied set of definitions for norms of minimum squared error (MSE).

Slepian [8] and [9] proved that the discrete motion blur models have a wide range of applications. McAdam [10] used a method of constrained deconvolution, using signals as sample sets and the matrix deconvolution models. He proved that all blurs can be mathematically modelled as a one dimensional filter. Mcadam [10] attributes this discovery of vector deconvolution by interspersing zeros to Preissendorfer. This model is similar to the present day projections onto convex sets.

Aboutalib et al. [11] used a theory, in which they implemented the impulse matrix as a combination of digital delay elements. The dynamical system representation of degradation due to motion blur was used. The dynamical system approach (state space approach) towards the blurring systems was pioneered by Silverman et al. [11] -

[13]. This approach allows the implementation of all the concepts of the dynamical systems theory to be applied to removal of motion blur.

Aboutalib [11] used the stability of any inverse filter as a guide to the rate of convergence and thereby improving the performance of the blur restoration filter. He termed the loss of information as a non causality of the blur restoration filter ( a term copied from the dynamical systems theory ).

Trussell et al. [14] - [18] developed the concepts of spatial domain filtering, like constraints analysis, feasible sets, eigenvalues of the impulse matrix, convergence, etc. Using the definition of PSF as a mapping function they defined restoration as inverse mapping onto the feasible set. To prove this they compared the performance of spatial domain filtering using minimization of least square error between the original signal and the signal estimate, with frequency domain techniques. They chose the feasible set as the exit point. They established similarities in performance and some theoretical links between these image restoration techniques.

Trussell, Civanlar and Hunt [14] - [18] established an empirical link between the convergence rate and the eigenvalues of the impulse matrix. They also proved that

the convergence criterion and the constraints had an effect not only on the path and the rate of convergence but also on the final solution. This meant that the feasibility of any technique depended on the assumptions made about the restoration. They also developed ad hoc techniques for the choice of the convergence criterion for the feasibility of any technique. These are very important results, since they constitute the guidelines as to how much constraints or assumptions any technique could allow without affecting the success of deblurring.

Tekalp et al. [37] conducted a comparative evaluation of the effect of different kinds of a priori information on different image restoration techniques. The performances of linear spatially invariant reduced update Kalman filter ( RUKF ), edge-adaptive RUKF and adaptive convex-type constraint based restoration implemented via the method of projection onto convex sets ( POCS ) were compared. They showed that spatially variant restoration methods namely the adaptive POCS algorithm and the edge-adaptive RUKF have a better potential to incorporate more a priori information into the final solution than the spatially invariant RUKF. They also proved that in the presence of noise the spatially invariant reduced update Kalman filter ( RUKF ) has a better performance. They concluded that numerous factors about the blur have to be considered before deciding the optimal image restoration technique.

Tekalp et. al. [38] developed a new decision-directed filtering algorithm for deblurring of images blurred by spatially variant motion blurs. They assumed that the spatially variant blur could be represented by a collection of distinct point spread functions. Each of these point spread functions were spatially invariant. A posteriori information was used to decide the method to split the blurred image. This method constituted a segmentation of the blurred image into regions of spatially invariant blurs. This algorithm saved the computation time required to deblur the blurred image by making use of faster algorithms available for spatially invariant blurs. They proved that the computation time could be further saved if the blurred image could be split into regions with no blurs in them. They confirmed that the technique succeeds when the blurred image consists of distinct edges or textures but fails to reliably deblur the flat regions in the blurred image.

Angwin et. al. [39] proposed a technique that reduced the computation time required for using Kalman filter on spatially variant blurs. The dimensions of the state space model for spatially variant blurs are very large. They proposed a reduced order model Kalman filter ( ROMKF ) which used a state space model with reduced dimensions. This was achieved by splitting the image into smaller regions thereby reducing the order of the impulse matrix. Thus the blurred image was effectively split into asymmetric regions with spatially variant blur. This approach enables the use of Kalman filters for adaptive image restoration.

Trussell [15] points out that all the iterative algorithms assume that a suitable starting point for iteration is either available or immaterial in deciding the success of that technique. He proved that this assumption is erroneous. He took two different starting estimates ( henceforth called the initial estimate ) and used the same constrained iterative restoration technique and found that one initial estimate was more successful than other. This question has been addressed in this thesis. An algorithm is developed, which does not depend upon any starting point. The algorithm generates a reliable starting point from the degraded signal for subsequent restoration.

Three image restoration techniques are studied in detail in the second chapter. The conclusions and results of these techniques are used to develop a new algorithm as mentioned earlier. The second chapter also presents the techniques used to identify the blur parameter.

The third chapter presents the new algorithm that was used successfully for restoring rigid body motion blur. This algorithm guarantees a good initial estimate for spatial domain iterative restoration. This reliability improves the performance of the restoration filter. It succeeded in restoring motion blurred images in the presence of additive noise with signal-to-noise ratio as low as 1.0. It had a fair performance for signal-to-noise ratio between 1.0 and

0.5. The robust nature of this algorithm was thus established. The implementation issues of this algorithm are also tackled in Chapter 3. This algorithm has an in built structure for a parallel hardware implementation, thus reducing the computational cost. The sensitivity of this algorithm to an error in the value of the blur parameter is studied. The last section of Chapter 3 provides the test results.

The fourth chapter provides the summary and the conclusion.

CHAPTER II  
IMAGE RESTORATION TECHNIQUES

2.1 Introduction

Three image restoration techniques are discussed in this Chapter. Their results are used by a new algorithm proposed in Chapter 3. These results are presented in Sections 2.3, 2.4 and 2.5, along with a brief introduction to the fundamentals involved in these three image restoration techniques.

A brief study of some of the important image restoration techniques which are to be used later is done in Section 2.6. A review of the techniques to find the value of the blur parameter is presented in Section 2.7. The uses and applications of other models like bilinear representation and multiple filter approach are discussed in Section 2.8. Section 2.9 gives the conclusions based on study done in this chapter.

2.2 Definitions

Terminologies specifically used in restoration of blurred images in spatial domain are defined in this section.

### 2.2.1 Constraints

Restoration of any blurred image has to satisfy certain mathematical conditions. These constraints may be on entire restoration ( for example, CPU time taken, implementation cost, etc. ) or on the signal or the signal estimate ( for example, continuity, pixel limits, contrast, good frequency resolution, etc. ) or on the noise ( for example, zero mean noise, noise spectrum, etc ). Each of these constraints have an inherent assumption about the process, which need not be universally true. The success of an image restoration technique depends on the amount and the validity of the constraints [2] and [14]. Excessive constraints may cause a failure ( for example, ringing ). Excessive constraints can be avoided by trial and error as proved in [2] and [14].

Hunt [17] analysed the effects of constraints on image restoration using the Mean Squared Error techniques. He concluded that it is generally useful to relax the constraints on the starting point in any iteration and then increase the number and the rigidity of the constraints, as the iteration approaches the final solution.

### 2.2.2 Projections Onto Convex Sets ( POCS )

A set  $C$  is convex, if for any two points  $x_1$  and  $x_2$



belonging to C, the point  $x_3$  given by the Equation ( 2-1 ) also belongs to C. A convex set C is defined as closed if it has finite boundaries. In this thesis closed convex sets with boundaries 0 and 255 are used.

$$x_3 = \alpha' x_1 + (1 - \alpha') x_2 \quad \dots\dots\dots ( 2-1 )$$

Where

$\alpha$  : is an number such that  $0 \leq \alpha' \leq 1$ .

$x_1$  and  $x_2$  : elements of a convex set C.

Trussell et al. [14] - [16] have shown that a constraint can be expressed in the form of a projection onto a convex set ( POCS ) i.e., a set of all the solutions satisfying that constraint. Let  $C_i$  be a closed convex set satisfying the  $i$ th constraint. Then the final solution is the one that satisfies all the convex sets, ie a solution belonging to the intersection of all the convex sets.

Let  $P_1$  be a projection operator which projects a solution onto a set, ie it implements the constraint on the convex set  $C_1$ . Then the starting point for the next iteration is as follows.

$$f^{n+1} = (P_1)(P_2) \dots (P_t) f^n \quad \dots\dots\dots ( 2-2 )$$

Where

$n$  : is the order of the iteration.

$f^n$  : is the signal estimate after  $n$  iterations.

$f^{n+1}$  : is the signal estimate after  $n+1$  iterations.

$t$  : the total number of constraints or the convex sets representing them.

$P_i$  : is the projection operator for the  $i$ th constraint ( $1 \leq i \leq t$ ).

Trussell et al. [14] - [16] have proved that the above equation converges and the final solution lies in the intersection of all the convex sets. This analysis has an advantage because the rigidity of any constraint can be controlled ( relaxed ) at any order of iteration by merely controlling the projection vectors without affecting the overall restoration process.

All constraints like variance and mean of the residual, pixel bounds, continuity etc., can be implemented as closed convex set. The proof for the above statement is given in Appendix B.

### 2.2.3 Feasible Set

A solution for the original image is defined as any technically possible solution for the original image. This just means that the probability that this solution might be the original image is not zero. A feasible solution is the one that satisfies all the constraints placed on it. This difference occurs because the probability that all the constraints placed on the solution are true, is not equal to one ( for example, the constraint of continuity, rigidity

etc., are not always true ).

Feasible set is a set containing all the feasible solutions. It is the intersection of all the closed convex sets  $C_i$ . Trussell et al. [14] have proved that the factors influencing the choice of a solution from the feasible set include the impulse matrix, noise, the rigidity of the convex sets and the initial estimate used to start the iteration.

#### 2.2.4 Convergence Rate, Path and Criteria

The rate of convergence is expressed in terms of number of iterative steps required to reach the final solution or the computational cost of the restoration. The path of convergence is the set of values taken by successive estimates.

The relations between the convergence rate and path with the constraints, noise and the eigenvalues of the impulse matrix were studied by Trussell [14] and [18], Sondhi [2] and Hunt [17]. A majority of their results are empirical, but they nonetheless hold for spatial domain iterative image restoration. These are briefly discussed in Section 2.4.

The convergence criterion is the mathematical function used to decide the exit from the iterations. It defines

whether or not the final solution has been reached. It need not always be the feasible set, since a lot of times it is necessary to exit in the vicinity of the feasible set ( for example, due to CPU time limit ). Generally the convergence criterion is a relaxed version of the feasible set as shown in Appendix C.

### 2.2.5 Eigenvalues and the Lost Information

The impulse matrix for motion blur is always singular. In other words there are always more variables than the equations a blur filter provides. Sondhi [2], Silverman et al. [11], Trussell et al. [14], Shim et al. [21] and Harris [4] have proved that the maximum rank of the impulse matrix is equal to the order of the degraded image. This proof for the case of a rigid body motion blur is given in Appendix D.

This loss of equations is expressed by a coefficient called the loss of information coefficient (LIC) defined as follows.

$$\text{LIC} = M / (\text{rank of } [H]) - 1 \quad \dots\dots\dots (2-3)$$

Where

M : the total number of variables to be found.

[ H ] : the impulse matrix.

The maximum rank of the impulse matrix [ H ], is equal to the order of the degraded image. In the case of motion

blur,  $M \geq$  the order of the degraded image. ( [2], [4], [11] and [14] ). Thus for motion blur  $LIC \geq 0$ .

This is also stated by Trussell [14] and Sondhi [2] as - " the maximum number of non zero eigenvalues of [ H ] is equal to N ". In practical cases there are some non zero eigenvalues in the vicinity of zero, thereby increasing the LIC. Trussell et al. [14] - [18] empirically established the relationship between the number of non zero eigen values in the vicinity of zero and the convergence rate. This proof is very briefly given in Appendix D.

#### 2.2.6 Continuity or Smoothness

This constraint, unlike non negativity is applied to the derivatives of the pixels. Appendix E gives the constraint of continuity on the higher order derivatives. It can be seen that non negativity and continuity involve the same equation, except that non negativity is implemented on pixel values while continuity is implemented on their derivatives.

#### 2.2.7 Dynamic range

This is an abstract term used to give a rough estimate of the number of the types of blurs ( or degradations in general ), which a given technique can solve successfully

where

$d$  : is the number of pixels moved by the rigid body.

In the case of an uniform motion the impulse response is as follows ( see Equation ( 1-10 ) ).

$$h(i) = \begin{cases} (1/d) & \text{for } -d + 1 \leq i \leq 0 \\ 0 & \text{else} \end{cases} \dots\dots\dots ( 2-5 )$$

Aboutalib et al. [11] state that motion blurs can be restored if the non causality of the impulse response is solved. A non causal filter in the time domain requires a future output to solve for a present output. But in a spatial domain approach for restoring motion blurs, this problem exists even if data from the past is required for restoration. This is because an image is a snapshot and data beyond the screen limits on all the four sides is not available. Thus in a spatial domain approach for restoring motion blurs, LIC ( given by Equation ( 2-3 ) ) is a more correct indicator of the lost information than the non causality of the impulse response.

Without loss of generality, denote  $h(i-d)$  as  $h_i$  and define  $z^1$  as the delay element of an arbitrary order  $i$  as follows.

$$z^1 f(x) = f(x-1) \dots\dots\dots ( 2-6a )$$

Thus Equation ( 2-4 ) can be written as a summation of

as used in [2] and [14].

### 2.2.8 Residual Outliers

In any spatial domain, iterative restoration constraints are implemented after every iteration [14]. Generally, after any iteration there are some pixels belonging to the signal estimate which does not satisfy the pixels limits given by Equation ( 2-1 ). These are called residual outliers.

### 2.3 A Dynamic System Model

This model was developed by Silverman et al. [11], [12] and [13]. It is a spatial domain technique which defines the impulse response as a collection of delay elements. In this section a dynamic system model is used to represent an 1-D linear and spatially invariant rigid body motion blur along the x direction.

In the absence of noise, Equation ( 1-2 ) can be rewritten for a linear and spatially invariant rigid body motion blur as in the x direction as follows.

$$g(x) = \sum_{i=0}^{d-1} h(i) f(x-i) \quad \dots\dots\dots ( 2-4 )$$

delay elements operating on  $f(x)$ .

$$g(x) = ( h_0 + h_1 z^{-1} + \dots + h_d z^{-d} ) f(x) \quad \dots\dots\dots ( 2-6b )$$

This is also used to define the blur filter as a tapped delay line operator.

if

$$H ( z^{-1} ) = h_0 + h_1 z^{-1} + \dots + h_d z^{-d}$$

then

$$g(x) = H ( z^{-1} ) f(x) \quad \dots\dots\dots ( 2-7 )$$

This is then represented by an equivalent single input single output linear difference system (  $A_1, B_1, C_1, D_1$  ) as in Equation ( 2-8 ). This is the dynamic system model ( state-space realization ) for a linear spatially invariant rigid body 1-D motion blur. Linearity and spatial invariance directly decide the properties of the state space matrices.

$$\begin{aligned} [ S_1 (x+1) ] &= [ A_1 ] [ S_1 (x) ] + [ B_1 ] [ f(x+d) ] \\ [ g (x) ] &= [ C_1 ] [ S_1 (x) ] + [ D_1 ] [ f(x+d) ] \end{aligned} \quad \dots\dots\dots ( 2-8 )$$

where

$S_1$  : is the state space vector for the dynamic system model.

$[ A_1 ]$ ,  $[ B_1 ]$ ,  $[ C_1 ]$  and  $[ D_1 ]$  are the state space matrices given in Figure 6.



Figure 6 gives the matrices and the state space vector set in terms of the elements of the impulse matrix and the pixels of the original signal.

This state space realization represents the blur at each line of the degraded image. This blur can be restored, if any one of the state space vectors is known. In the absence of noise, this would give a complete recovery of the original signal. This result was used in the algorithm proposed in Chapter 3. The order of state space vector  $[ S1(x) ]$  is equal to the blur parameter.

Restoration in a noise free case can also be accomplished by employing the recursive inverse of the dynamical model given in Equation ( 2-8 ), ie the set of state space matrices (  $[ A2 ]$ ,  $[ B2 ]$ ,  $[ C2 ]$ ,  $[ D2 ]$  ) as follows.

$$\begin{aligned} [ S2 (x+1) ] &= [ A2 ] [ S2 (x) ] + [ B2 ] [ g (x) ] \\ [ f(x+d) ] &= [ C2 ] [ S2 (x) ] + [ D2 ] [ g (x) ] \\ &\dots\dots\dots ( 2-9 ) \end{aligned}$$

Where

$$\begin{aligned} [ A2 ] &= [ A1 ] - [ B1 ] [ D1 ]^{-1} [ C1 ]^T \\ [ B2 ] &= [ B1 ] [ D1 ]^{-1} \\ [ C2 ] &= - [ D1 ]^{-1} [ C1 ] \\ [ D2 ] &= [ D1 ]^{-1} \end{aligned}$$

$[ A1 ]$ ,  $[ B1 ]$ ,  $[ C1 ]$  and  $[ D1 ]$  are the state space

$$\begin{aligned}
 [A_1] &= (1/h_0) \begin{bmatrix} 0 & -h_2 & \cdot & \cdot & -h_d \\ 0 & 0 & \cdot & \cdot & 0 \\ \cdot & h_0 & \cdot & \cdot & \cdot \\ \cdot & \cdot & h_0 & \cdot & \cdot \\ \cdot & \cdot & \cdot & h_0 & 0 \end{bmatrix}_{d \times d} \\
 [B_1] &= \begin{bmatrix} h_1 \\ -h_0 \\ 0 \\ \cdot \\ \cdot \end{bmatrix}_{d \times 1} \\
 [C_1] &= \begin{bmatrix} 1 & 0 & \cdot & \cdot & 0 \end{bmatrix}_{1 \times d} \\
 [D_1] &= \begin{bmatrix} h_0 \end{bmatrix}_{1 \times 1} \\
 [S_1(x)] &= \begin{bmatrix} h_1 f(x+d-1) + h_2 f(x+d-2) + \dots + h_d f(x) \\ -h_0 f(x+d-1) \\ -h_0 f(x+d-2) \\ \cdot \\ \cdot \\ -h_0 f(x) \end{bmatrix}_{d \times 1}
 \end{aligned}$$

Figure 6. The Dynamical Model ( State-Space ).

matrices given in Figure 6. The assumption that  $h_0$  is not equal to zero ensures the existence of an inverse.

#### 2.4 Generation of Information from Background Pixels

Sondhi [2] proved that the blur can be removed if the lost information is estimated. Sondhi [2] and Slepain [9] proposed an algorithm in which this lost information is derived by the information about the background pixels. They used a priori information to decide the values of the background pixels. Sondhi [2] stated that the above approach failed due to the inaccuracy of the a priori information. The algorithm proposed in the next chapter uses a very reliable method to find this lost information.

#### 2.5 The Landweber Iteration

Landweber's equation is one of the most profoundly used equations for iterative applications. Trussell [14] and [18] applied it to blur restoration. Landweber's iteration is an algorithm that defines every iterative step in an iteration, which starts from a random starting point.

The motion blur in matrix notation (see Equation (1-3)) can be rewritten as follows.

$$[g] - [h][f] = 0 \quad \dots \dots \dots (2-10)$$

For an arbitrary order of iteration  $\phi$  the next point can be found using equation ( 2-11 ). For convenience the matrix notations are neglected.

$$[ f^{\phi+1} ] = [ f^{\phi} ] + [ f^{-\phi} ]$$

and

$$[ f^{-\phi} ] = [ L ] [ h ]^t ( [ g ] - [ h ] [ f^{\phi} ] )$$

..... ( 2-11 )

Where

[ L ] : is a matrix which alters the convergence properties but not the final solution. This matrix is dependent on the impulse matrix. The elements of this matrix are obtained depending upon how the convergence properties are to be altered.

[ h ]<sup>t</sup> : is the transpose of the impulse matrix.

[ f<sup>ϕ</sup> ] : is the estimate of the original signal [ f ] after ϕ iterations.

[ f<sup>ϕ+1</sup> ] : is the estimate of the original signal [ f ] after ϕ+1 iterations.

[ g ] : is the degraded signal in a matrix notation.

Trussell [18] proved that in case of blur this iteration converges to a solution obtained by the technique of singular value decomposition of the impulse matrix. This is also the solution obtained by using the mean squared error technique, in the absense of additive noise. The strength of the landweber's equation lies in the fact that it could be

applied in any domain.

Trussell et al. [14] proved that for a motion blurred image to be restored, the final solution has to belong to the same feasible set. Since the feasible set is independent of image restoration techniques, Trussell et al. [14] proved that the final solution of all successful image restoration techniques belongs to the same feasible set, as long as the impulse matrix is not altered. The proposed algorithm uses the same impulse matrix as that of the blur filter. Thus, if the algorithm is successful, then the final solution would belong to the same feasible set as all other image restoration techniques. The difference is that the algorithm skips the singular part of the impulse matrix and uses only the non singular part.

## 2.6 Some of the Important Image Restoration Techniques

In this section four different image restoration techniques are studied. Each of these techniques has started a new direction in the field of image restoration. They have influenced all the subsequent research in this field. A brief outline of these techniques is done so as to provide a rationality to the assumptions made regarding motion blurred images in this thesis.

### 2.6.1 Minimization of the Mean Squared Error ( MSE )

The method of minimizing mean squared errors between two signals ( the original signal and the signal estimate for this thesis ) [1] - [9] is of a great significance because many techniques have revolved around this approach. Slepian [8] - [9], Sondhi [2], Harris [3] - [4], Horner [5] - [6] and Helstrom [7] were among the first to investigate this approach to the problem of image restoration.

The optimum path in this iteration is defined as the path which optimizes the objective function ( for example, cost, time taken, etc. ). Optimization techniques are used to select the best path of iteration.

Slepan [8] - [9] and Sondhi [2] have done research linking the rank of the impulse matrix and the loss of information on the original image. Harris [3] - [4] and Horner [5] - [6] studied the effects of replacing the true impulse matrix with a matrix whose properties were altered as per the requirements of the restoration. They used an approximate invertible matrix, a matrix with a bad overall noise performance but a better noise performance in frequency ranges noticeable to human eye, etc. But all the above researchers derived the information required to restore the blurred image from the additional assumptions made regarding the motion blur. Thus their approaches failed

on blurs when these assumptions did not hold true.

### 2.6.2 Conditional Expectation

Helstrom [7] used the conditional expectation of the original signal given the noise and the degraded signal for restoring blurred images. This technique combines statistics with restoration in a unique manner. A brief outline of this method is given below.

Let the original signal  $[ f ]$ , noise  $[ n ]$  and the degraded signal  $[ g ]$  be a set of random processes  $\{ f \}$ ,  $\{ n \}$  and  $\{ g \}$ , respectively. Then an estimate of  $f$  ( $f^\circ$ ) could be obtained using mean squared error technique as in section 2.6.1. This estimate is obtained by minimising  $E_c$  as follows.

$$E_c = E [ ( f - f^\circ )^2 ] \quad \dots\dots\dots ( 2-12a )$$

Where

$E_c$  : is the expectation over  $\{ f \}$  and  $\{ n \}$  processess.

The blurred image is restored if  $E_c$  is known. Let  $e^-$  denote the error between the original signal and its estimate and let  $E_d$  denote the conditional expectation of  $e^{-2}$  given  $\{ g \}$  and  $\{ n \}$ . Then  $E_d$  is a random variable whose expectation over the process  $\{ g \}$  ensemble gives  $E_c$ . Then  $E_c$  is minimized by minimizing  $E_d$ .

But

$$E_d = E [(f-b)^2/g] + E [(f-b)^2/g] \dots\dots\dots ( 2-12b )$$

where

$$b : \text{ is the conditional expectation } E [ f/g ].$$

So  $E_c$  is minimized if

$$f = b = E [ f/g ] \dots\dots\dots ( 2-12c )$$

Equation ( 2-12c ) looks very simple to implement. But the problem lies in the fact that computing the conditional expectations for any random processes ( { n } and { g } in this case ) is very difficult.

### 2.6.3 Singular Value Decomposition ( SVD )

The impulse matrix representing the motion blur filter is always non singular. In singular value decomposition method, the restoration is attempted by manipulating the eigenvalues of the impulse matrix till it is made invertible, i.e., non singular ( by approximation or estimation ) [2], [21] and [22]. But a restoration of any motion blur is extremely sensitive to the composition of the impulse matrix. Thus singular value decomposition involves a trade off between signal quality and noise performance as shown in [2] and [21]. The notion of separating the impulse matrix into two parts, non singular and singular is derived from the principles involved in the singular value



decomposition method.

The singular value decomposition methods differ on the ways to operate on these eigenvalues. In truncated singular value decomposition method, eigenvalues are manipulated by replacing all the eigenvalues below a threshold to some constant [21]. In stochastic singular value decomposition method, eigenvalues are manipulated by replacing the eigenvalues with values zero ( or in the vicinity of zero ) with values derived from the stochastic processes { g } and { n } [21].

The main drawback of these techniques is that even for a matrix of an order as small as 10 finding the eigenvalues is a computationally enormous task. This is true for impulse matrices of rigid body motion blurs.

#### 2.6.4 Inverse Filtering

A convolution of two signals in the time domain corresponds to a multiplication of their responses in the frequency domain. Multiplication is invertible by division. Since the degraded image, in the case of a rigid body motion blur, is a convolution of the impulse response and the original image ( see Equations ( 1-1 ) and ( 1-2 ) ), the original image can be obtained from Equation ( 2-13 ) and Equation ( 2-14 ). Here the frequency response of the

original signal is obtained by dividing the frequency responses of the degraded signal and the impulse response. The original signal can be found by taking an IFFT of the frequency response of the original signal ( Equation ( 2-14 ) ). This is the main principle behind inverse filtering [1a] - [2]. Generally noise is assumed to be absent.

$$G(u,v) = H(u,v) F(u,v) + N(u,v) \quad \dots\dots\dots ( 2-13 )$$

Where

$G(u,v)$  : is the frequency response of the degraded signal.

$F(u,v)$  : is the frequency response of the original signal.

$H(u,v)$  : is the frequency response of the motion blur filter.

$u$  and  $v$  : are the frequencies in the  $x$  and  $y$  direction respectively.

Thus the restored signal is given by Equation ( 2-14 ).

$$\begin{aligned} \hat{f}(x,y) &= \text{IFFT} \{ G(u,v)/H(u,v) \} \\ &= f(x,y) + \text{IFFT} \{ N(u,v)/H(u,v) \} \\ &\quad \dots\dots\dots ( 2-14 ) \end{aligned}$$

There are two main drawbacks of this technique. Since for any rigid body motion blur, the impulse matrix is always singular. Thus the division by these zeros is avoided by approximation or estimation of the impulse response. Since

signals are very sensitive to small changes in their frequency response, this gives rise to a non-existent noise [2]. The second drawback relates to noise sensitivity. Noise generally has a uniform spectrum, while the impulse response has very low values in the high frequency range. This acts as a noise amplifier [2].

There have been many techniques which have tried to overcome these drawbacks. But all of them place certain additional assumptions and constraints on the restoration process.

## 2.7 Data Extraction Techniques ( Blur parameter )

An accurate estimate of blur parameter is a very important part of restoration of motion blurs. In this section a brief review of some prominent techniques for estimating the blur parameter is presented. These are implemented in the three domains, namely, the frequency domain, the cepstrum domain and the spatial domain.

### 2.7.1 Frequency Domain Approach

In the absence of noise, Equation ( 2-13 ) proves that, the zeros of  $H(u,v)$  are the zeros of  $G(u,v)$ . The loci of the zeros of the impulse response are a function of the blur parameter. Assuming that  $F(u,v)$  has no zeros, the loci of

the zeros of  $G(u,v)$  are used to estimate the blur parameter [2].

The main drawback of the data extraction techniques in the frequency domain is that the zeros of the impulse matrix are highly noise sensitive.

### 2.7.2 Cepstrum Domain Approach

Cannon [31] proposed an algorithm which used an averaging technique in the cepstrum domain. The cepstrum of the degraded signal is averaged over windows of the orders similar to the blur parameter of the motion blur. In this method it is assumed that the cepstrum of the original signal has a zero mean. Thus this operation would then give a cepstrum having the characteristics of the cepstrum of the impulse response.

This is a definite improvement over the frequency domain techniques. But this technique still is very noise sensitive. This technique makes an additional assumption about the cepstrum of the original image having a zero mean.

### 2.7.3 Spatial Domain Approach

The spatial domain methods consists of finding the equation of motion. The equation of motion ( linear or non

linear ) can then be used to obtain the blur parameter and thus, the impulse matrix. The success of this approach depends upon the generation of the equation of motion from the blurred image. Since the blur parameter and the impulse matrix are obtainable from the equation of motion for any type of motion blur.

Broida et al. [24] used a recursive technique to get the equation of motion by modeling the object dynamics as a function of time. But a large amount of data analysis is involved even for a simple motion. Broida et al. [24] also proposed a method of improving the performance by using an iterated extended Kalman filter to handle this complexity. This however failed to improve the performance in data extraction. A large amount of data analysis makes the spatial domain approach for data extraction extremely difficult.

## 2.8 Multiple Degradations

In this thesis a single source of blur is assumed, namely, a rigid body motion blur. Sometimes more than one source of blur causes the degradation. This results in multiple degradations. Though this was not a part of the problem addressed in this research, it is important to study the prominent models for multiple blurs. Two models are briefly presented for such blurs.

### 2.8.1 Double Convolution Model ( Cascading of blurs )

If the impulse responses of the two blurs are  $h_1(i,j)$  and  $h_2(i,j)$  respectively then Equation ( 2-15 ) gives the double convolution model ( see [1] and [34] ).

$$g(x,y) = \sum_{i=-\infty}^{+\infty} \sum_{j=-\infty}^{+\infty} h_1(i,j) g_m(x-i,y-j)$$

such that,

$$g_m(x,y) = \sum_{i=-\infty}^{+\infty} \sum_{j=-\infty}^{+\infty} h_2(i,j) f(x-i,y-j) \dots\dots\dots ( 2-15 )$$

Where

$g(x,y)$  : is the degraded signal.

$f(x,y)$  : is the original signal.

$h_1(i,j)$  : is the impulse response of the first blur.

$h_2(i,j)$  : is the impulse response of the second blur.

In nature this type of degradation occurs very rarely [20]. Any spatially invariant blur and spatially variant blur of the same type of source does not follow cascading. This definition of same type of sources of blur is a subjective definition.

The double convolution model has a high noise creation, i.e., the inversion process creates noise where none

existed. In the absence of noise, let  $n_1 \{ \}$  and  $n_2 \{ \}$  be the errors introduced due to deblurring by  $Ih_1 ( )$  and  $Ih_2 ( )$ , respectively. Here deblurring by  $Ih_1 ( )$  and  $Ih_2 ( )$  are defined as restorations used to deconvolve  $h_1(i,j)$  and  $h_2(i,j)$  respectively. It is not important how the deblurring is done since the effect of doing both the deblurrings simultaneously on the same blurred signal is being presented.

Since the restoration is independent of the order [20], blur can be removed by first inverting  $Ih_1 ( )$  and then  $Ih_2 ( )$  as given in Equation ( 2-16 ).

$$\begin{aligned} Ih_1(g) &= gm \\ &= gm + n_1\{g\} \end{aligned}$$

So,

$$\begin{aligned} Ih_2( Ih_1(g) ) &= Ih_2( gm ) + Ih_2( n_1\{g\} ) \\ &= f + n_2\{gm\} + Ih_2( n_1\{g\} ) \end{aligned} \quad \dots\dots\dots ( 2-16 )$$

### 2.8.2 Bilinear Model

Leahy et al. [20] proposed a bilinear model to overcome the difficulties in cascading two sources of blurs. A single output double input bilinear response was modified by Leahy et al. [20] to get a suitable representation for blurs as follows. This is a single output single input representation

of motion blurs with two sources.

$$g(x: x_1, x_2) = \int_{x_2=-\infty}^{+\infty} \int_{x_1=-\infty}^{+\infty} q(x_1, x_2) f(x_1) f(x_2) dx_1 dx_2 \quad \dots\dots\dots ( 2-17 )$$

Where

$q(x_1, x_2)$  : is the double impulse response of the bilinear filter.

$f(x_1)$  : is the original image as a function of co-ordinate  $x_1$ .

$f(x_2)$  : is the original image as a function of co-ordinate  $x_2$ .

The bilinear model given by Equation ( 2-17 ) has more applications than the double convolution model. However a computer simulation and specifically a parallel hardware implementation is difficult for any bilinear model.

## 2.9 Conclusions

The dynamical system model ( state-space approach ) used by Silverman et al. [11] - [13] guarantees a complete signal recovery if one state-space vector is provided. It does not however specify any source to generate a state-space vector. Sondhi [2] and Slepian [9] proposed an algorithm in which they generated this lost information from the back ground pixels. But this method is very unreliable. The landweber iteration is a very powerful tool for restoration of a



degraded signal. The properties of convergence of spatial domain iterative techniques were established from this algorithm ( see [14] - [18] ).

Four important techniques were presented in Section 2.6. The fundamentals of image restoration established by these techniques have been incorporated in the research relating to this thesis.

Data extraction methods were briefly presented in Section 2.7. The spatial domain method was found to be least useful for the purpose of blur parameter extraction. All the data extraction methods are shown to be very unreliable. The technique proposed by Cannon [31] could be used as an Pre-restoration analysis to further improve the performance of any blur restoration.

The conclusions of the image restoration techniques analysed in this chapter are used to develop a new algorithm in the next chapter.

## CHAPTER III

### RESTORATION BY REVERSE MAPPING

#### 3.1 Introduction

In this chapter an algorithm for the restoration of images blurred by motion is presented in detail. The restoration is done using the non singular part of the impulse matrix. The lost information is generated from the behaviour of the closed convex sets at the pixel boundaries.

In the absense of noise, Silverman et al. [11] - [13] established that ( for a linear model of motion blur ) the exact original image could be found, if the lost information is available. Trussell et al. [15] and [18] proved that an iterative image restoration with a non singular impulse matrix had a high rate of convergence. Sondhi [2] and Slepian [9] proved that in the case of rigid body motion blurs, the errors in estimates generated from iterative restoration can be expressed in terms of the lost information ( i.e., the pixels out of the scope of the camera ). The proposed algorithm incorporates all these results in restoring images degraded by rigid body motion blur.

The success of this algorithm has been proved for rigid body motion blur in x and xy direction. The performance of

this algorithm for finding the blur parameter has also been tested. The algorithm yields good results in the presence of additive noise with SNR ( signal to noise ratio ) as low as 1.00. Here SNR is defined as the ratio of the variances of the two signals namely the original signal and the additive noise.

The above algorithm is discussed in detail for restoration of images degraded by rigid body motion blur with constant velocity.

### 3.2 Rigid Body Uniform Linear Motion Blur

Rigid body motion blur could be in any direction including along the z direction. Unless specified, this chapter deals with motion in the x direction. Relative velocity between the camera and the object is assumed to be constant.

The blur model depends upon the assumptions made about the motion blur. The convolution model representing a motion blur filter, given by Equation ( 1-3 ) is used in this chapter. The impulse matrix [ h ] is assumed to be a square ( M x M ) matrix. This is done by extending the degraded signal  $g(x,y)$  by  $d-1$  zeros along the x direction. Equation ( 3-1 ) is the blur filter for one dimensional rigid body motion blur in the x direction.

$$g(x,y) = \sum_{i=0}^{d-1} (1/d) f(x+i,y) + n(x,y)$$

for all  $x$  and  $y \in [1,N]$  ..... ( 3-1 )

where

$d-1$  : is equal to the number of pixels moved. The value of  $d$  is assumed to be known.

$g(x,y)$  : is the degraded signal.

$f(x,y)$  : is the original signal.

$n(x,y)$  : is the additive noise.

The positive sign in the convolution is obtained by shifting the original signal by the number of pixels moved [13]. Note that for  $d = 1$ , there is no motion blur. Since the motion blur Equation ( 3-1 ) is independent of the  $y$  axis, the notation  $y$  will be neglected for  $x$  direction motion blur in this chapter.

As established earlier, in case of rigid body motion blur, the impulse matrix is singular [2] and [8] - [18]. Thus inversion in any domain is not possible without certain approximations or estimations.

In frequency domain the singularities are in the form of zeros of  $H(\exp\{j\Omega\})$ . In order to avoid a division by zero they either have to be approximated or estimated. This approximation gives rise to noise amplification, especially

for the high frequencies. The human eye has been proved to be very sensitive to high frequency components of an image ( [2], [34] and [35] ). All the image restoration techniques implemented in the frequency domain involve such approximations or estimations as illustrated in [2].

In spatial domain the singularity of the impulse matrix means that there are more signal variables to be solved than the number of equations available. The number of independent equations in Equation ( 3-1 ) is equal to the rank of [ h ] ( N in this case ). The number of signal variables of the original signal ( f(x) in this case ) to be solved is equal to  $N + d - 1$ . This can be clearly seen in Equation ( 3-2 ), which calculates the number of equations required to restore the blurred image.

The number of equations available = N

The number of variables of the original signal f(x) = M

i.e., The number of equations required for deblurring = M

Since,

$$M = N + d - 1 \quad \dots\dots\dots ( 3-2a )$$

i.e.,  $M > N$ . Thus, there is a loss of information.

A loss of information can be better given by the LIC ( loss of information coefficient ) [25]. In this thesis LIC is defined by equation ( 3-2 ).

$$\text{LIC} = (M)/N - 1 = (N+d-1)/N - 1 = (d-1)/N$$

..... ( 3-2b )

Motion blur given by Equations ( 3-2a ) and ( 3-1 ) has infinite solutions. Thus for a uniform linear rigid body motion blur, the feasible set is not a null set. Sondhi [2], Trussell [14], Hunt [17], Tekalp et al. [25] and Oja et al. [26] have all proved that in case of a uniform linear rigid body motion blur, the feasible set is a null set only if too many constraints are placed on the image restoration or too many assumptions are made about the image degradation.

The new algorithm proposed requires the estimation of  $d-1$  pixels. This makes the impulse matrix non singular. The degraded image is then restored using the inverse of a non singular matrix or the dynamical systems model ( state-space approach ) proposed by Silverman et al. [11]. This has advantages, since the impulse matrix used for restoration has no approximations. The impulse matrix used for restoration represents the motion blur as in the blur model.

The estimation of  $d-1$  pixels of the  $f(x)$  should not be random. Since a random estimation is highly inaccurate. This would nullify the advantages of using a non singular impulse matrix for inversion.

This estimation is done by using a property of closed

convex sets given by Equation ( 3-3 ). Motion blurs are in the form of moving averages ( averaging due to motion ) mapped onto a closed convex set ( pixel bounds ). Thus if any pixel of the blurred signal  $g(x)$  is equal to 0 or 255 then all pixels of the original signal  $f(x)$ , contributing to  $g(x)$  have to be 0 or 255, respectively ( in the absence of noise ).

Let  $g(x_0) = 255$  ( or 0 ) for  $0 \leq x_0 \leq 255$ .

In the absence of noise Equation ( 3-1 ) gives,

$$g(x_0) = (1/d) ( f(x_0) + f(x_0+1) + \dots + f(x_0+d-1) )$$

But  $f(x)$  satisfies Equation ( 1-5 ), thus,

$$0 \leq f(x_0), f(x_0+1), \dots, f(x_0+d-1) \leq 255.$$

Only one set of values for  $f(x)$  satisfies the above two conditions as shown in Equation ( 3-3 ).

$$f(x_0) = f(x_0+1) = \dots = f(x_0+d-1) = 255 \text{ ( or 0 )} \\ \dots\dots\dots ( 3-3 )$$

Equation ( 3-3 ) is true for all  $x \in [1, N]$ .

( for example, if  $g(20) = 255$ . Then

$$g(20) = (1/d) ( f(20) + f(21) + \dots + f(20+d-1) )$$

and  $0 \leq f(20), f(21), \dots, f(20+d-1) \leq 255$

$$\Rightarrow f(20) = f(21) = \dots = f(20+d-1) = 255 \quad ).$$

There are now  $N-1$  remaining independent equations and  $N-1$  pixels of the original signal to be found. This is always possible. The algorithm postulates that - " Even though finding a degraded pixel with boundary values 255 or 0 is hard, a degraded pixel in some boundary of 255

( or 0 ) exists ". So an estimation similar to Equation ( 3-3 ) can be done at the location of a pixel which is nearest to the pixel limits given by [0,255].

This pixel belonging to the degraded set is nearest to the pixel bounds and is called the boundary pixel. The boundary function used to select the location of the boundary pixel is as follows.

$$B'(x) = \min (g(x); 255-g(x)) \quad \dots\dots\dots ( 3-4 )$$

Where

$B'(x)$  : is a function that evaluates the shortest distance of any pixel from the pixel bounds.

$g(x)$  : is the degraded signal.

$B'(x)$  is a set of  $N$  numbers. Therefore from the maxima and minima theory it has a minimum. Without a loss of generality let it be at  $x_0$ .

$$\text{i.e., } \min (B'(x)) = B'(x_0) \quad \text{for all } x \in [1, N]$$

Similar to Equation ( 3-3 ) assign the estimates as  $f(x_0) = f(x_0+1) = \dots = f(x_0+d-1) = g(x_0) \dots\dots\dots ( 3-5 )$

Statistically for any number  $\sigma$ , there is a finite probability for the existence of at least one element of the degraded signal  $\in [255-\sigma, 255]$  ( or  $[0, \sigma]$  ). Thus the estimation given by Equation ( 3-5 ) is done at the pixel nearest to the boundary given by [0,255]. The smaller the



number  $\sigma$ , the more accurate is the estimation given by Equation ( 3-5 ).

For random boundary limits  $[255-\sigma, 255]$ , let  $p(\sigma)$  be the probability that it has at least one degraded pixel and let  $q(\sigma)$  be the probability that estimation given by Equation ( 3-5 ) is correct within limits acceptable by some arbitrary criteria.

Then as  $\sigma \rightarrow 0$ ,  $p(\sigma) \rightarrow 0$  and  $q(\sigma) \rightarrow 1$ . Thus using the estimation given by Equation ( 3-5 ) restoration is done as follows.

$$f(x_0+d) = d g(x_0+1) - \{ f(x_0+1) + \dots + f(x_0+d-1) \}$$

$$\begin{array}{c} \cdot \qquad \qquad \cdot \qquad \qquad \cdot \qquad \qquad \cdot \\ f(N+d-1) = d g(N) \quad - \{ f(N) \quad + \dots + f(N+d-2) \} \end{array}$$

and

$$f(x_0-1) = d g(x_0-1) - \{ f(x_0) \quad + \dots + f(x_0+d-2) \}$$

$$\begin{array}{c} \cdot \qquad \qquad \cdot \qquad \qquad \cdot \qquad \qquad \cdot \\ f(1) \quad = d g(1) \quad - \{ f(2) \quad + \dots + f(d) \quad \quad \quad \} \end{array}$$

..... ( 3-6 )

In the restoration given by Equation ( 3-6 ) noise was assumed to be absent. This is not true for a majority of motion blurs. Moreover, the pixels at the boundaries are more noisy. Thus the boundary function has to be protected against picking up locations of noisy pixels.

For example let a part of the degraded signal be

$x_{o-3} \ x_{o-2} \ x_{o-1} \ x_o \ x_{o+1} \ x_{o+2}$

{ ..... 127, 132, 129, 255, 121, 118, ..... }.

If  $x_o$  is chosen as the location of the pixel used for estimation by Equation ( 3-6 ), the restoration will produce wrong results. Such failures in this estimation can be avoided by pre-restoration noise filtering or by redefining the boundary function to skip a possible noisy pixel. The former approach would not filter all the noisy pixels and would lead to a loss of the blur model ( Sondhi [2], Trussell et al. [18] and Slepian [9] ). A small improvement in the definition of  $B'(x)$  gives a very good performance as can be seen from the results given in Section 3.7.

This is done by introducing  $E(g/n)$  as an expectation of  $\{ g \}$  given  $\{ n \}$ . This insures that no noisy pixels are selected for the estimation given by Equation ( 3-6 ). The boundary function is given by

$$B(x) = B'(x) + \alpha E(g/n) \quad \text{..... ( 3-7a )}$$

where

$\alpha$  : is a coefficient given by equation ( 3-7b )

$E(g/n)$  : is an algorithm which decides whether  $g(x)$  is noisy or not ( a binary function using the statistical expectation  $E(g/n)$  ).

$$\begin{aligned} \alpha &= 0 && \text{if } g(x) \text{ is not noisy} \\ &= 128 && \text{if } g(x) \text{ is noisy} \quad \text{..... ( 3-7b )} \end{aligned}$$

Sondhi [2] established that the probability of a noisy pixel being near 255 is not equal to the probability of a noisy pixel being near 0. This is incorporated in the boundary function  $B(x)$ , by giving a weighted coefficient for both the boundaries. This had to be done to improve performance of the restoration in the blurred photograph of the robber ( see Figure 13 ). The boundary function is then given by Equation ( 3-8 ).

$$B(x) = \min [ a_l g(x) ; a_h ( 255-g(x) ) ] \\ + a E (g/n) \quad \dots\dots\dots ( 3-7c )$$

where

$a_l$  and  $a_h$  : are weighted coefficients used to decide the a white or a black boundary pixel. Unless specified both are equal to 1.

Let  $f_0(x)$  be the initial estimate given by Equation ( 3-6 ). Let the error in this estimate  $f_0(x)$  be given by  $u(x)$ . Then  $u(x)$  is given by Equation ( 3-8 ).

$$f(x) = f_0(x) + u(x) \quad \text{for all } x \in (1,M) \\ \dots\dots\dots ( 3-8 )$$

But both  $f(x)$  and  $f_0(x)$  satisfy the blur model given by Equation ( 3-1 ). Using Equations ( 3-1 ) and ( 3-6 ) a relation between individual elements of  $u(x)$  is found.

$$\sum_{j=0}^{d-1} u(x+j) = 0 \quad \dots\dots\dots ( 3-9a )$$

Thus

$$u(x) = u(x+d) = - \sum_{j=1}^{d-1} u(x+j) \quad \dots\dots\dots ( 3-9b )$$

Thus in the case of rigid body motion blur, the error in the initial estimate is periodic with the blur parameter. This property gives a strong control over the noise generated. ( In the presense of additive noise this summation would be a function of the standard deviation of noise ).

But the initial estimate does not satisfy the constraints. The pixel boundary limit and the continuity constraint is implemented on this estimate. The final result obtained from implementing both these constraints is the restored signal.

To impose the constraint given by the pixel limits, define  $v(x)$  as in Equation ( 3-10 ). The function  $v(x)$  gives the extent by which any individual pixel estimate overshoots the pixel limits given by Equation ( 1-5 ).

$$v(x) = \begin{cases} -f_0(x) & \text{if } f_0(x) \leq 0 \\ 255 - f_0(x) & \text{if } f_0(x) \geq 255 \\ 0 & \text{else} \end{cases} \quad \dots\dots\dots ( 3-10 )$$

where

$v(x)$  : is a function defined to impose the pixel limit constraint on the estimate of  $f(x)$ .

Then the next estimate is as follows.

$$f_1(x) = f_0(x) + v(x) \quad \dots\dots\dots ( 3-11a )$$

Where

$f_1(x)$  : is an estimate of the original signal satisfying the constraint of pixel limits.

$f_0(x)$  : is an estimate of the original signal satisfying the blur model given by Equation ( 3-1 ).

The new estimate  $f_1(x)$  does not satisfy the blur model given by Equation ( 4-1 ). This means that  $f_1(x)$  does not satisfy the periodicity of the error, given by Equation ( 3-9 ).

Thus the next estimate  $f_2(x)$  is found by imposing the error control Equation ( 3-9 ) on the estimate  $f_1(x)$ . This is done in a similar manner to the initial estimation model given by Equation ( 3-6 ).

Let the next estimate be given by Equation ( 3-11b ). Note that since  $u(x)$  is periodic with a period  $d$ , it suffices to find just the first  $d$  elements of  $u_1(x)$ . But for this assumption to work the highest error in all the periodic locations has to be taken into account. This is

illustrated in an example and in Equation ( 3-12 ).

$$f_2(x) = f_1(x) + u_1(x) \quad \dots\dots\dots ( 3-12a )$$

where

$u_1(x)$  : is given by Equation ( 3-12b ).

There are  $d-1$  independent elements of  $u_1(x)$ . These are found by imposing equation ( 3-12a ) on  $u_1^-(k)$ .

$$u_1(k) = u_1^-(k) - 1/(d-1) \sum_{j=0}^{d-1} u_1^-(j)$$

for  $0 \leq k \leq d-1$  and  $j \neq k \quad \dots\dots\dots ( 3-12b )$

where

$$u_1^-(k) = \begin{array}{ll} \max [ v(k+id) ] & \text{if all } v(k+id) \geq 0 \\ \min [ v(k+id) ] & \text{if all } v(k+id) \leq 0 \end{array}$$

for all  $0 \leq i \leq \text{int}(M/d)$

Note that  $v(x+id)$  has the same polarity for all values of  $i$ , since an underestimation of  $f(x)$  means an underestimation of  $f(x+d)$  and so on. This property is due to the periodicity of  $u(k)$  and  $u_1(k)$ .

The periodicity of  $u(x)$  is the main factor giving a solid control over the generated noise. This periodicity is due to the use of the exact blur matrix. This periodicity is lost by any approximation of the inverse matrix.

The estimate  $f_2(x)$  given by Equation ( 3-11 ) and

( 3-12 ) may not satisfy the pixel limits. Thus a solution for the original signal  $f(x)$  is found in a recursive manner. The results of this algorithm on an image degraded due to motion blur are presented in Section 3.7 in detail. This algorithm was also implemented on motion along a direction at an angle of  $45^\circ$  with the  $x$  axis. This recursive algorithm could also be implemented with different constraints. This is a possible area for further research.

{

For example let  $u_1^-(0) = 30, u_1^-(2) = \dots = u_1^-(10) = 0$

Assuming  $N = 128$  and  $d = 11$ , ie  $M = 138$ .

From equation ( 3-12 ) on  $u_1^-(k)$  gives

$$u_1(0) + u_1(2) + \dots + u_1(10) = 0$$

By using the technique used in the algorithm of equal distribution we have,

$$u_1(0) = 30$$

$$u_1(1) = -3$$

$$. = -3$$

$$u_1(10) = -3$$

But from Equation ( 3-9 )

$$10$$

$$u(11) = - \sum_{j=1}^{10} u(0+j) = u(0)$$

$$j=1$$

& so on for all  $x \in (1, M)$  }

But the error control sets  $u(x), u_1(x)$  and  $v(x)$  are not

signals. They are corrections in the estimates of the original signal. Hence the signal constraints cannot be implemented on them. This problem cannot be solved for any random motion blur. But for the case of uniform linear motion blur these error control sets can be expressed in terms of signal variables of  $f(x)$ . Sondhi [2] has proved that for rigid body motion blur, Equation ( 3-13 ) can be used.

$$f(x) = \sum_{i=0}^L g'(x+id) + \phi(j) \quad \begin{array}{l} 1 \leq j \leq d \\ \dots\dots\dots ( 3-13 ) \end{array}$$

where

$$L = \text{int} ( (N-x)/d )$$

$$j = (L+1) d + x - N$$

$$g'(x) = g(x) - g(x+1) \quad ( \text{at } x = N \quad g'(x) = g(N) )$$

$\phi(j)$  has the same periodicity as  $u(x)$ .  $\phi(j)$  denotes the part of the signal outside the scope of the camera. Since the set is a part of the original signal, all the constraints can also be imposed on this set. Thus for a uniform linear rigid body motion blur, the error sets can be imposed with all the signal constraints.

{ Sondhi [2] has proved that

$$\begin{aligned} \phi(j) &= f(N+j) & j \neq d \\ & & d-1 \\ &= \sum_{jj=1} f(N+jj) & j = d \end{aligned}$$

}



This algorithm involves a technique of reverse mapping. Here the pixels of the original signal contributing to a degraded pixel are mapped to the pixels of the blurred image. The pixels of the original signal are then evaluated by functions that depend upon the pixels of the degraded signals in the mappings. In the next section this algorithm involving reverse mapping is implemented on a general degradation.

The results of this algorithm in restoring linear spatially invariant rigid body motion blurs are presented in Figures 8, 9, 10, 11, 12 and 13. The success of this algorithm in restoring motion blurred images is seen from these results.

### 3.3 General Degradation

The algorithm proposed in Section 3.2 can also be used for any given general degradation assuming that the general degradation is in the form of the convolution model given by Equation ( 1-3 ). To establish the use of this algorithm for any degradation, this algorithm will be conceptually applied to a blur with impulse matrix  $[ h ]$ . Thus only those Properties which are independent of the impulse matrix are used in this section.

The boundary function given by Equations ( 3-7 ) is

independent of the degradation. Using Equations ( 3-7 ), a set of boundary values given by  $B(x,y)$  should be found.

Define

$$P_1 = (x_1, y_1)$$

such that

$$\min_1 ( B(x,y) ) = B(x_1, y_1) \quad \text{for all } x \text{ and } y \in [1, N] \\ \dots\dots\dots ( 3-14 )$$

where

$P_1$  : is the first location selected or the first order selection point.

Let  $S_i$  be the set of locations of the pixels of  $f(x,y)$  contributing to the boundary pixel of  $g(x,y)$ , from the  $i$ th order selection. This is obtained by reverse mapping through  $[ H ]$ . But for a general degradation all the non zero elements of  $[ H ]$  are not equal. Thus all the members of  $S_i$  do not have equal contribution. A criterion to decide the locations with more energy contribution is used. This criterion is called the Weighted Selection Criterion (WSC).

Let

$$Q = \sum_{k=0}^M \sum_{j=0}^M h\phi(k, l) \\ \dots\dots\dots ( 3-15 )$$

where

$\phi$  : denotes the reverse mapping. This can be evaluated from the definition of the set  $S_i$ .

Then the Weighted Selection Criterion ( WSC ) is given by the equation ( 3-16 ). The set  $S'1$  is a subset of the set  $S1$ .

$$WSC = (1/Q) \sum_{k=1}^M \sum_{j=1}^M h\phi'(k,l) \dots\dots\dots ( 3-16 )$$

where

$\phi'$  : denotes a subset of the reverse mapping. This can be evaluated from the definition of the set  $S'1$ .

From Equations ( 3-15 ) and ( 3-16 ) it can be proved that  $0 \leq WSC \leq 1$ .

$\phi'$  denotes reverse mapping through the locations of [ H ] corresponding to the set  $S'1$ . The location members of  $S'1$  are selected from the members of  $S1$ . This selection is based on the decreasing order of values of [ H ].

Thus only those pixels of the original signal contributing more energy to  $g(x1,y1)$  are picked up by  $S'1$ . While all the pixels contributing to  $g(x1,y1)$  are picked up by  $S1$ .

$S'1$  is defined as follows.

If

$(k',l') \in S'1$  and

$(k,l) \in S1$  and

$(k,l) \notin S'1$

Then

$$h\phi(k,l) \leq h\phi'(k',l') \quad \text{for all } h\phi(k,l) \in \beta_1$$

..... ( 3-17 )

Let V be the number of signal elements lost. Then repeat the above process j times. This would give j locations of the boundary function from Equation ( 3-13 ), i.e., P1, P2, ... Pj. If r1, r2, ... rj be the number of members of β'1, β'2, ... β'j, respectively.

Then the algorithm exits after j selections.  
such that

$$V \leq \sum_{i=1}^j r_i$$

$$V > \sum_{i=1}^{j-1} r_i$$

( Note that in the case of a rigid body motion blur in one direction,  $V = (LIC) N$  ) ..... ( 3-18 )

where

- LIC : is the loss of information coefficient.
- N : total number of pixels of the degraded image.
- V : total pixels lost.

Here all the β'i sets are exclusively independent by definition.

The Weighted Selection Criterion WSC are the criterion which decide the noise control. All the constraints are similarly implemented on the restoration as in the one dimensional rigid body motion. Thus the sets  $S_i$  define the locations where the initial estimation given by Equation ( 3-6 ) is done. The degraded image is then restored in a recursive manner.

### 3.4 Implementation Issues

In this section the implementation issues of the algorithm proposed in Section 3.2 are tackled.

#### 3.4.1 Parallel Hardware Implementation

The computation and the production cost of any algorithm can be drastically reduced if the algorithm lends itself to parallel computations. This allows the hardware of the circuit to be set up with a parallel logic. Thus the existence of any parallel structure in an algorithm is an important issue.

The error control given by Equation ( 3-9 ) and the correction sets  $u(x)$ ,  $u_1(x)$  and  $v(x)$  are examples of parallel structured data. This feature can be implemented on a parallel hardware. This saves a lot of time and gives this algorithm an added advantage. Figure 7 gives the parallel

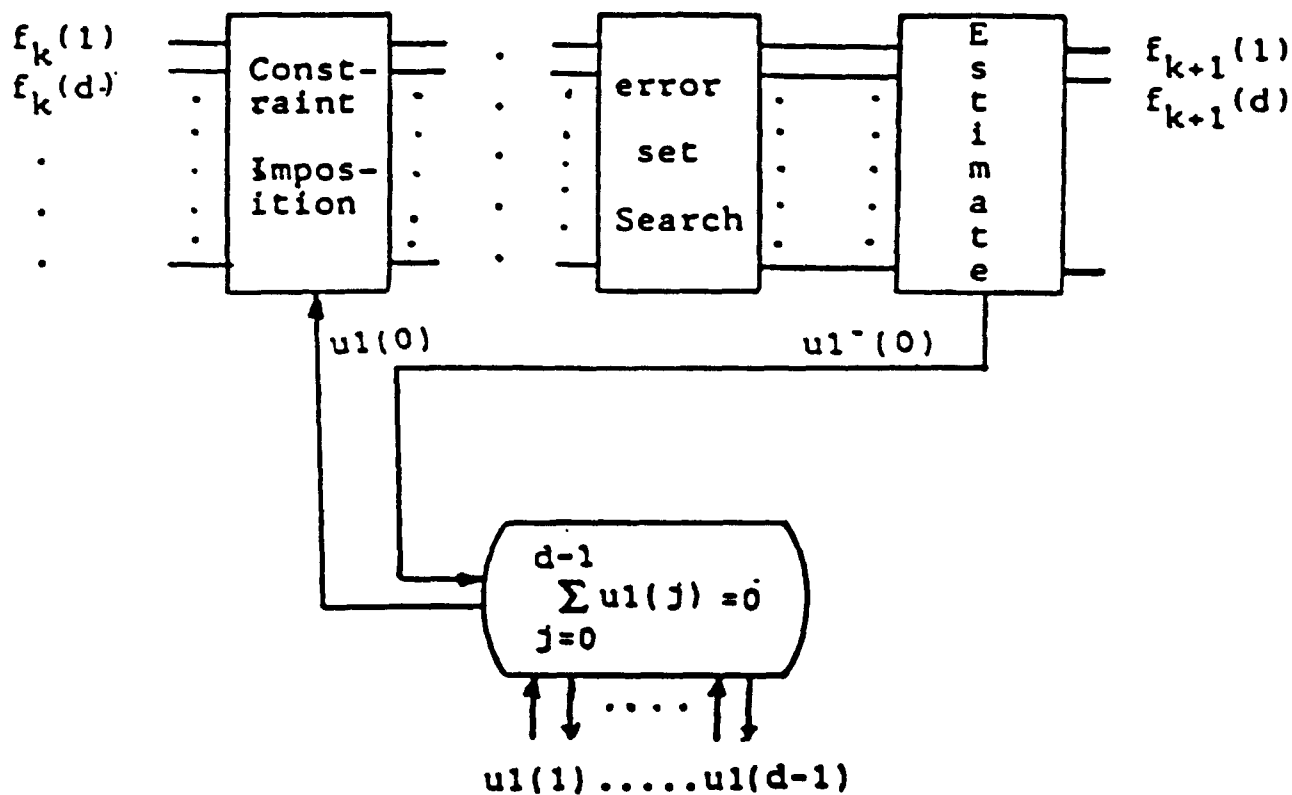


Figure 7. Parallel Hardware Implementation

hardware implementation.

### 3.4.2 Noise Sensitivity

The success of any image restoration algorithm depends upon the sensitivity of the algorithm to the presence of noise. The performance of this algorithm in restoring motion blurred images in the presence of additive noise, with SNR as low as 1.00, is seen to be good. The results are provided in Figure 13.

The reverse mapping algorithm has a provision for rejecting noisy pixels. This is achieved by implementing the noise shield given by Equation ( 3-7 ). This had a fair success in restoring images with SNR as low as 1.00. In the presence of noise, the noise control equation given by Equation ( 3-9 ) is modified as stated earlier.

### 3.4.3 Blur Parameter Estimation

The blur parameter is never available in real life images blurred by motion. Data extraction techniques are used in finding the blur parameter. These data extraction techniques are highly unreliable as stated earlier. The reliability of the reverse mapping algorithm proposed in Sections 3.2 and 3.3 can be used to overcome this problem.

Assume that an algorithm succeeds in restoring a degraded image. Then the blur parameter sensitivity is defined - " as the maximum percentage of error in the value of the blur parameter, for which this algorithm still succeeds in restoring the degraded image ". The algorithm was experimentally established to have a blur parameter sensitivity of 3%. This suggests that a failure ( in some extended form ) of this algorithm could be used to predict the blur parameter.

#### 3.4.4 Constraints

In spatial domain techniques the constraints are very important factors in deciding the success of the image restoration technique ( Trussell [18], Hunt [17] and Sondhi [2] ). Ringing is an example of the effects of excessive constraints. Ringing could however be avoided by relaxing these constraints ( [2], [17] and [18] ) by trial and error. The problem of excessive constraints exists for image restoration techniques. This is a drawback in automating the relaxation of constraints, since this requires user interaction. The error control Equation ( 3-9 ) provides a good method through which the constraints could be controlled in an automated application of image restoration.



### 3.4.5 Kalman Filtering

Aboutalib et al. [11] proposed a method in which they utilized a Kalman-Bucy filter to solve for complex spatially variant motion blurs. For a degraded image, multiple estimates are obtained. Then the actual estimate is found by taking a weighted average of all the estimates.

The capability of the Kalman-Bucy filter to handle computationally complex restoration is used. Such statistical approaches could also be used with the reverse mapping algorithm proposed in Section 3.2. This operation would however lose all the parallel structures, since Kalman filters are complex in structure and hence generally cannot be implemented on a parallel hardware structure. Kalman filters also do not guarantee stability. Hence Aboutalib [11] proposed that Kalman filters be used for very complex blurs where all other techniques are either too cumbersome or have failed to restore.

### 3.5 Advantages and Drawbacks of Reverse Mapping Algorithm

The algorithm has a lesser number of calculations compared to the image restoration techniques studied in this thesis ( for example, the image restoration techniques given in [2], [7], [10], [18], etc. ). The algorithm has a very strong control over the generated noise, ( Equation. ( 3-9 ) )

as seen in the results. This is a direct result of using the non singular part of the impulse matrix. The algorithm has an inherent parallel software. As stated earlier this allows the implementation of parallel hardware. This generates savings in terms of computation and production costs.

The use of the error control equation and the simplicity of this algorithm allows it to succeed in restoring motion blurs with LIC in the range of 50%. This is a big improvement as compared to other image restoration techniques ( for example, 12.5% in [2], 2.5% in [11], 15% in [26], etc. ). A good performance of this algorithm, in the presence of additive noise with SNR as low as 1.00, proves that the algorithm is robust. This algorithm makes very basic and few assumptions as compared to other image restoration techniques ( for example, [2], [7], [18], [21], etc. ). This makes it possible to use this algorithm in diverse applications.

The algorithm proposed in Sections 3.2 and 3.3 has very few drawbacks. These drawbacks did not have any effect on restoration of computer simulated blurs. But the drawbacks of this algorithm had an effect on the restoration of robber's blurred face as can be seen from Figure 13.

The algorithm utilizes a straight response to start the estimation process. Thus it has weak noise control for

frequencies smaller than the blur parameter. This is because in the initial estimate these values are put to zero. This can however be avoided by assuming a different set of response. Sondhi [2] has proved that such decisions rely on a priori information. Hence this drawback will exist in any kind of response used in estimation.

This algorithm is computationally very simple for motion blurs. The computational simplicity of this algorithm is not guaranteed for any general degradation. The computation cost of this algorithm is a function of the complexity of the impulse response. However this algorithm is computationally much simpler than the image restoration techniques discussed in Chapter 2.

### 3.6 Conclusions

In this chapter a reverse mapping algorithm was proposed for restoration of images degraded by uniform linear rigid body motion blur. This algorithm preserves the blur model. This is a major deviation from the conventional image restoration techniques.

The results of these experiments are presented in the next section. The summary and conclusions drawn from the results presented in the next section are given in Chapter 4. Chapter 4 also discusses the possibilities of further

research.

### 3.7 Results

All the images used in this thesis are of the size 128 x 128. Figures 8, 9, 10 and 11 consist of sets of images of a chessboard, a piston, toys and a dollar bill respectively.

Each of the above set consists of an original image, a pair of motion blurred images and their respective deblurred images. The blurred images in Figures 8, 9, 10 and 11 were obtained by computer simulation of the blur filter for motion along x direction (image (b)) and along a direction making an angle of  $45^\circ$  with the x axis (image (c)), respectively. The values of the blur parameters  $d$ , for the images blurred by motion along x direction, in Figures 8, 9, 10 and 11, are 50, 45, 20 and 45 respectively. The values of the blur parameters  $d$ , for the images blurred by motion along a direction making an angle of  $45^\circ$  with x axis, in Figures 8, 9, 10 and 11, are 50, 35, 30 and 35 respectively. These blurred images were restored by implementing the algorithm proposed in Section 3.2 and 3.3. Image (d) in Figures 8, 9, 10 and 11 consists of the deblurred image for blur along x direction. Image (e) in Figures 8, 9, 10 and 11 consists of the deblurred image for blur along a direction making an angle of  $45^\circ$  with the x axis.

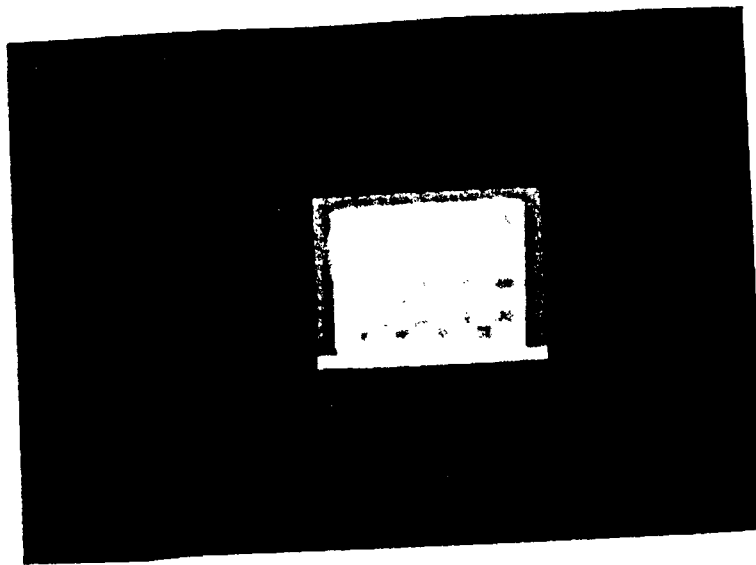
Figure 12 consists of three motion blurred images of a dollar bill corrupted with noise and their respective restored images. The blurring and noise corruption was done by computer. Additive sand paper noise was used in Figure 12. The value of the blur parameter  $d$  in all the three blurred images is 35. In Figure 12 the signal-to-noise ratio for the blurred images (a), (c) and (e) are 3.0, 1.0 and 0.25, respectively. The restored images for (a), (c) and (e) are images (b), (d) and (f), respectively. The results shown in the Figure 12 are obtained after relaxing the error control equation ( 3-9 ).

Figure 13 gives the results of implementing this algorithm on a real life blurred robbers image (image (a)). The algorithm failed in the bottom half of the image due to the failure of the linear model given by Equation ( 3-1 ). Hence the bottom part of the restored image was substituted to make the restored image more recognizable (image (b)). The histogram of the restored image was further equalized (image (c)) to bring out the salient features of the robber's face. This image was provided by Royal Canadian Mounted Police, Windsor. This image has been taken from a robbery scene recorded in a convenience store in Windsor.

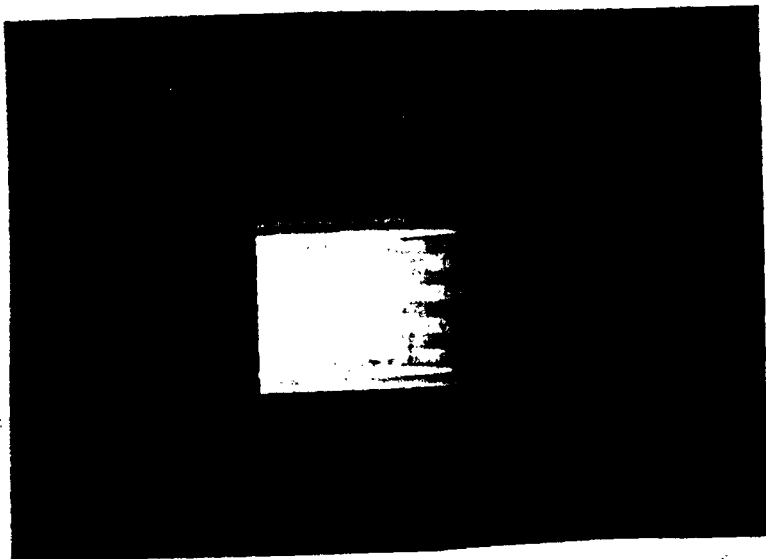
Figure 14 gives the results of implementing this algorithm with a wrong value of the blur parameter  $d$ . The

image of a chess board was blurred by computer with a blur parameter of 30. The algorithm was then implemented with blur parameter values of 10 (image (a)), 20 (image (b)) and 40 (image (c)) representing errors of -66%, -33% and +33%, respectively. All the above attempts failed in restoring the blurred images. Thus the blur parameter sensitivity of the algorithm from the above set of images is 1 pixel out of 30, i.e., 3%. These results show that the algorithm is very sensitive to the blur parameter.

Figure 15 consists of a set of images of the face of a lady. This set of images consists of an original image, a motion blurred image and the deblurred image. The pixels of this original image are evenly distributed over the grey scale. The blurred image (image (b)) was obtained by computer simulation of the blur filter for motion along the x direction. The value of the blur parameter is 40. Image (c) is the deblurred image which was obtained by implementing the algorithm proposed in Section 3.2 and 3.3.



(a)

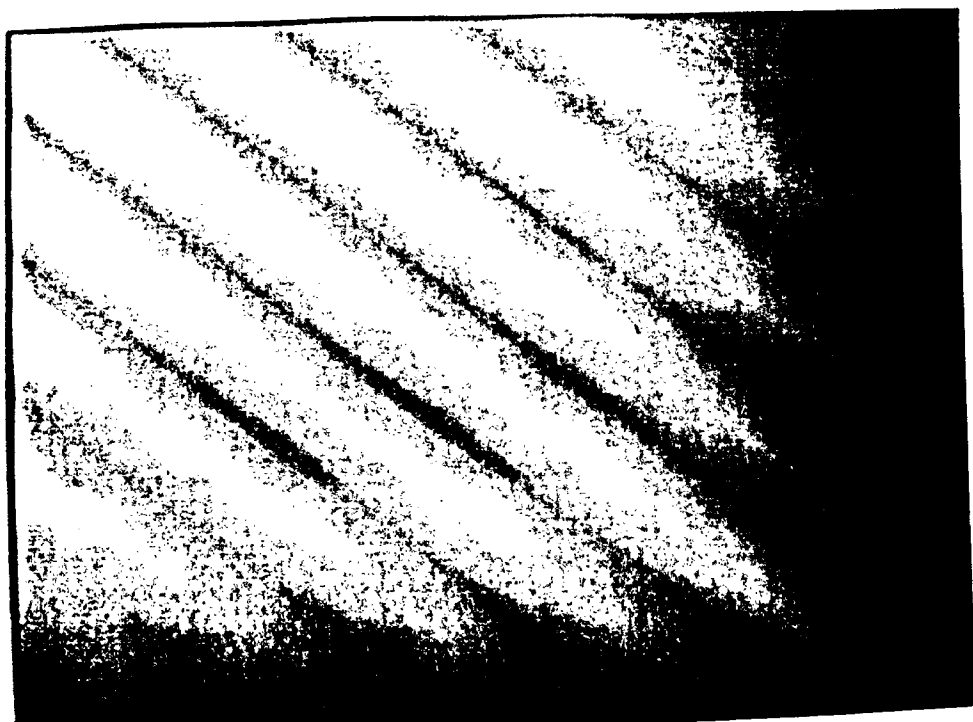


(b)

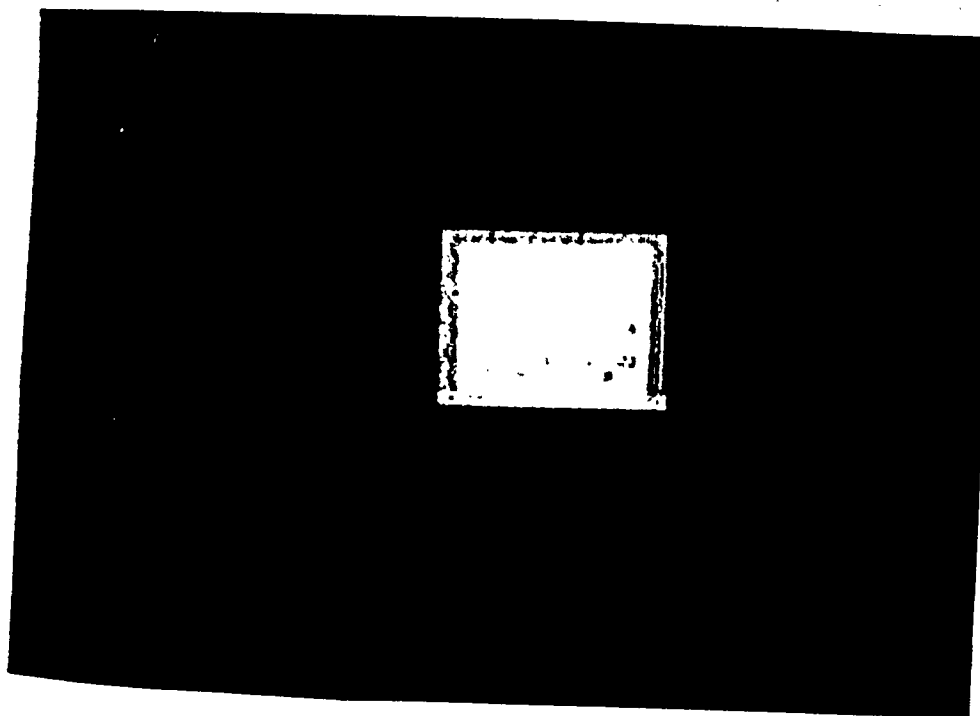
**Figure 8. Set of Images of a Chessboard**

- (a) The original image.
- (b) The blurred image with  $d = 50$  and  $\theta = 0$ .
- (c) The blurred image with  $d = 50$  and  $\theta = 45^\circ$ .
- (d) The deblurred image obtained by implementing the reverse mapping algorithm on image (b).
- (e) The deblurred image obtained by implementing the reverse mapping algorithm on image (c).

Where  $d$  is blur parameter and  $\theta$  is the angle between the direction of motion and the  $x$  axis.

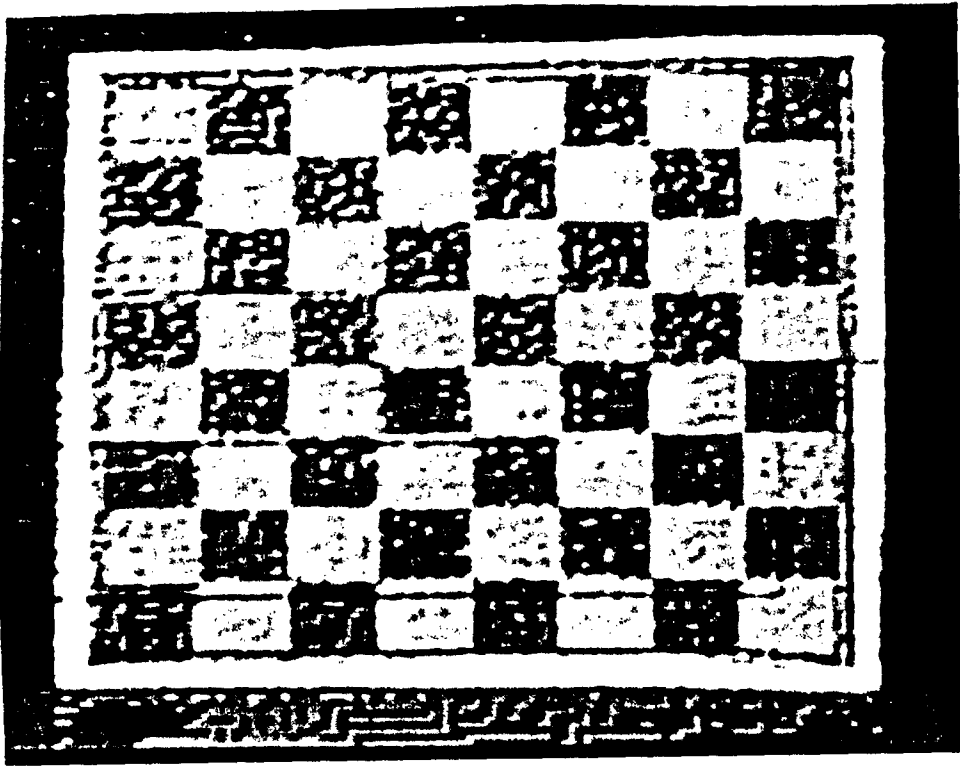


(c)

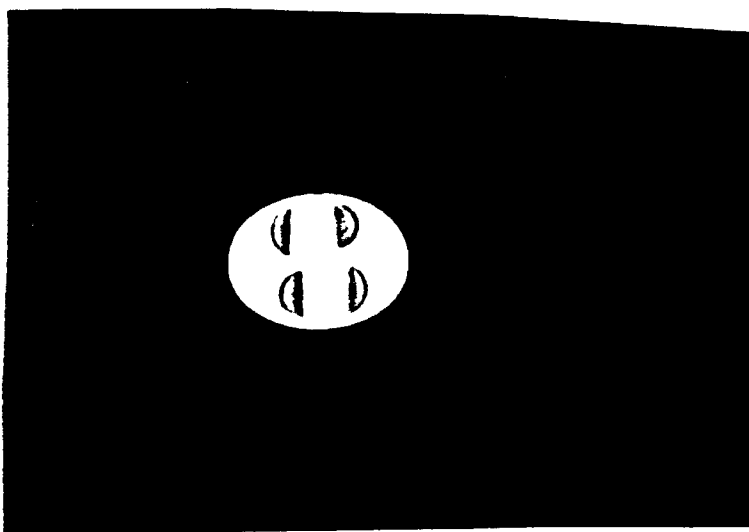


(d)

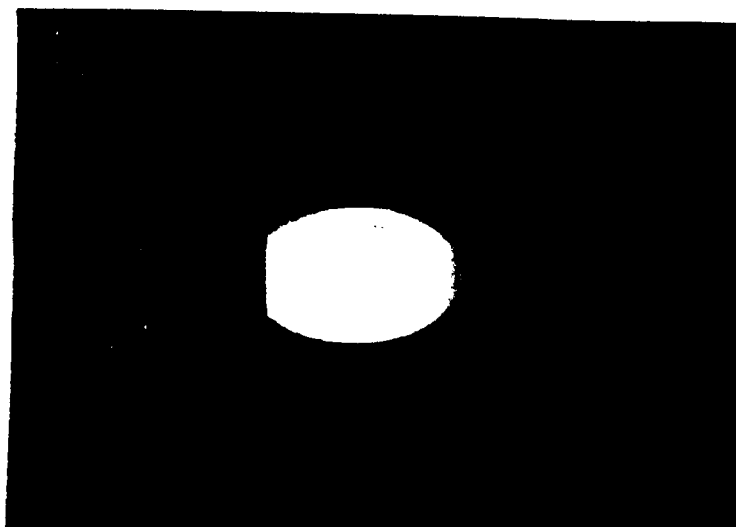




(e)



(a)



(b)

**Figure 9. Set of Images of a Piston**

(a) The original image.

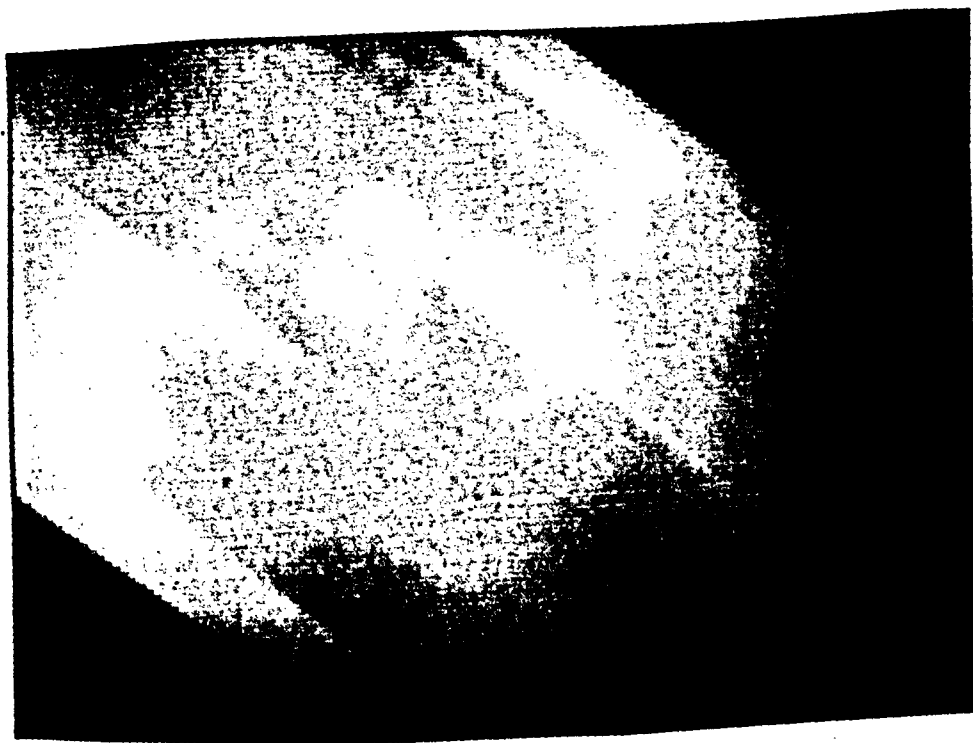
(b) The blurred image with  $d = 45$  and  $\theta = 0$ .

(c) The blurred image with  $d = 35$  and  $\theta = 45^\circ$ .

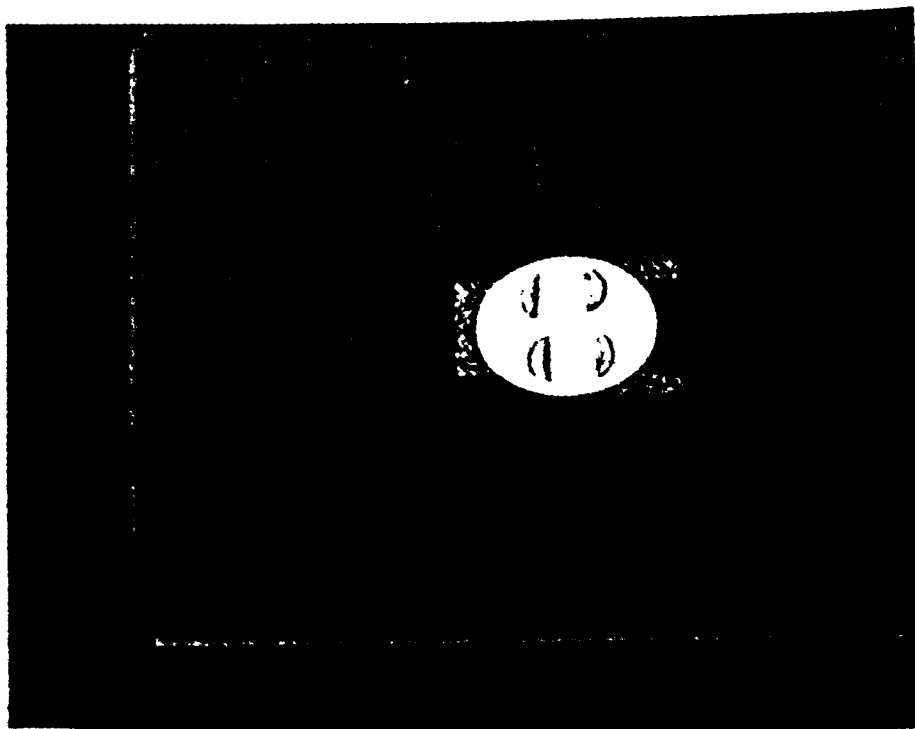
(d) The deblurred image obtained by implementing the reverse mapping algorithm on image (b).

(e) The deblurred image obtained by implementing the reverse mapping algorithm on image (c).

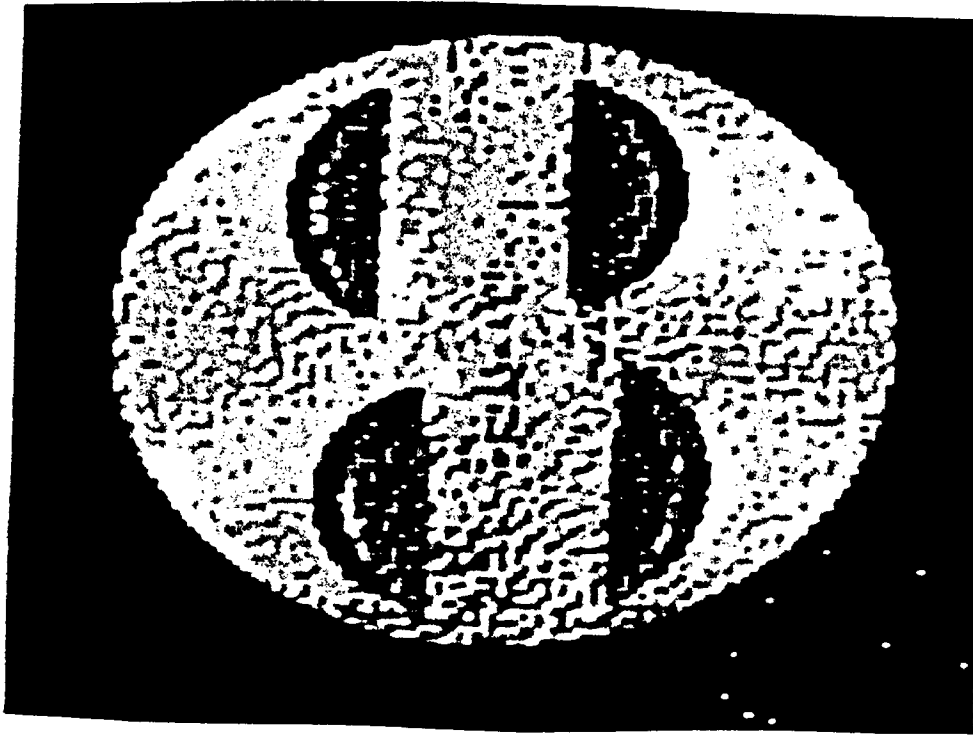
Where  $d$  is blur parameter and  $\theta$  is the angle between the direction of motion and the  $x$  axis.



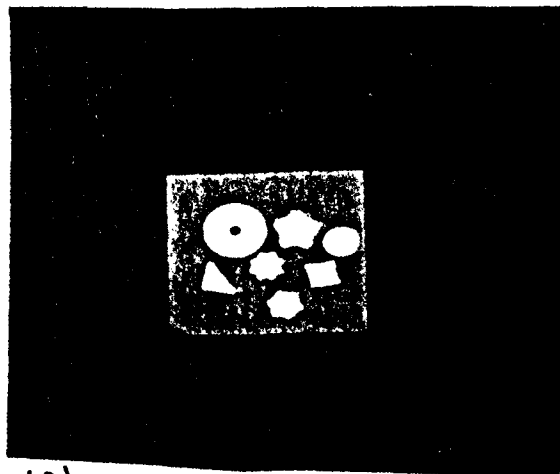
(c)



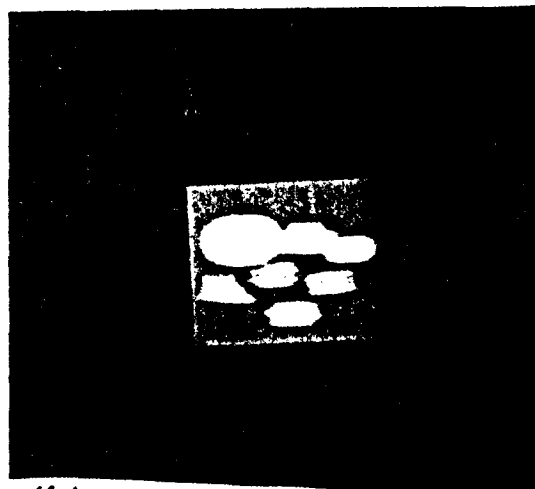
(d)



(e)



(a)



(b)

Figure 10. Set of Images of Toys

(a) The original image.

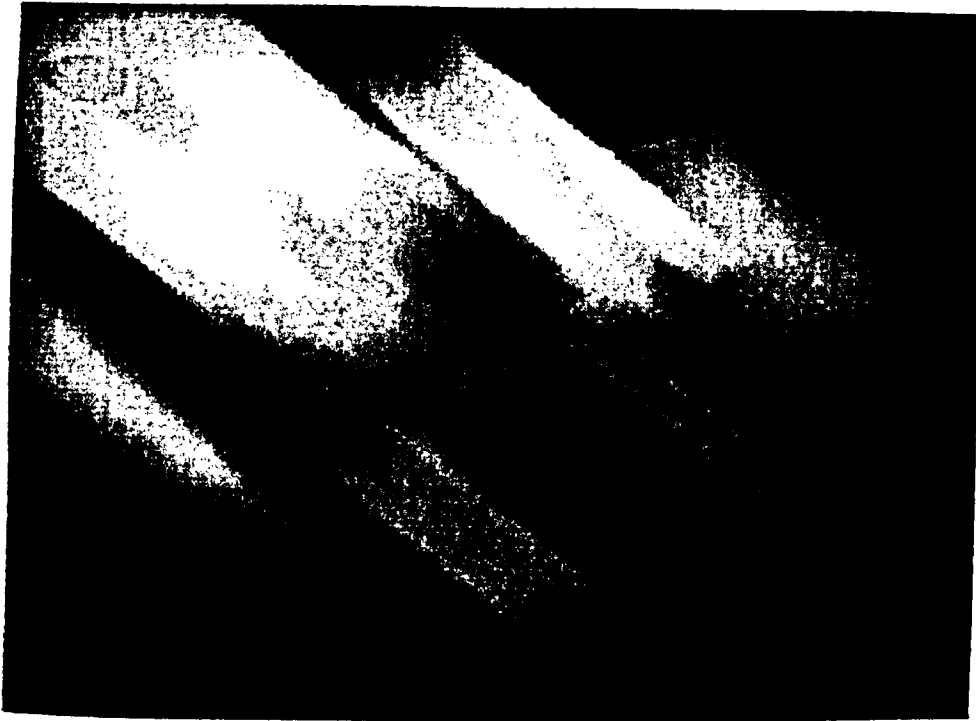
(b) The blurred image with  $d = 20$  and  $\theta = 0$ .

(c) The blurred image with  $d = 30$  and  $\theta = 45^\circ$ .

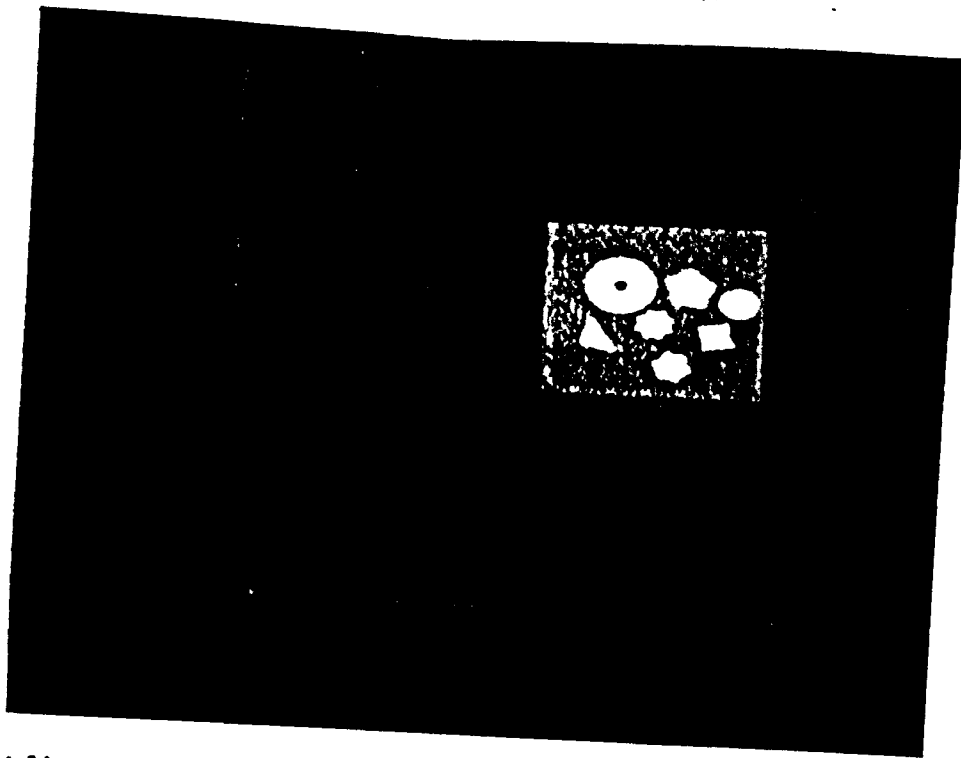
(d) The deblurred image obtained by implementing the reverse mapping algorithm on image (b).

(e) The deblurred image obtained by implementing the reverse mapping algorithm on image (c).

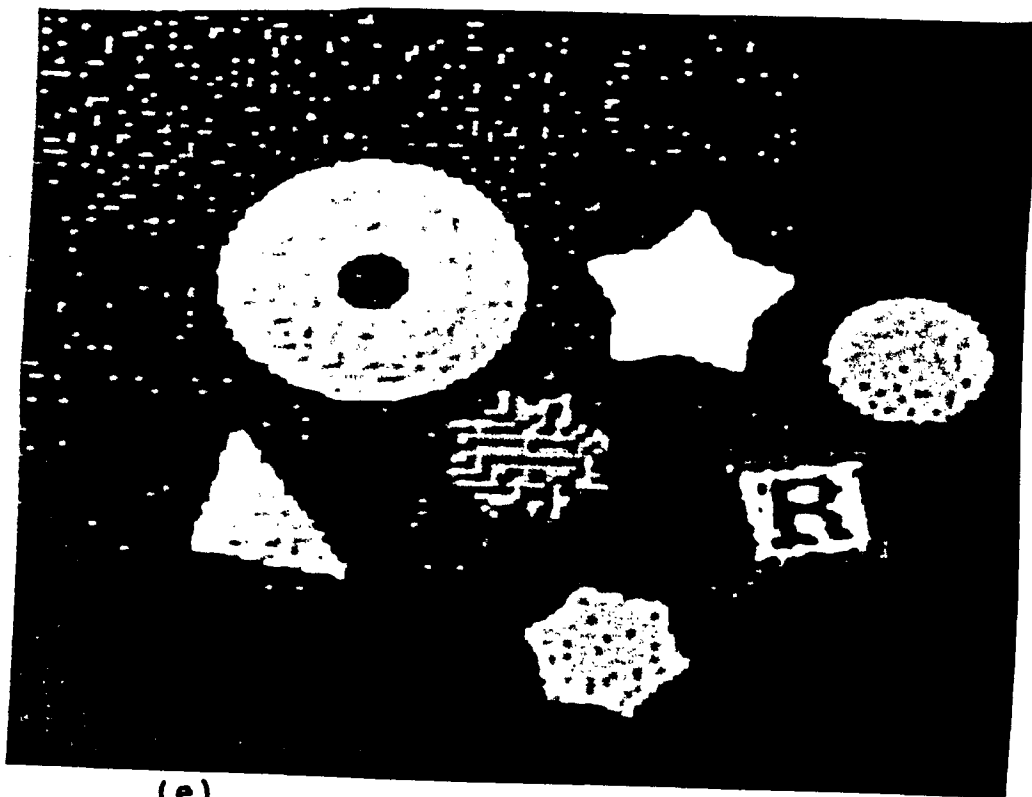
Where  $d$  is blur parameter and  $\theta$  is the angle between the direction of motion and the  $x$  axis.



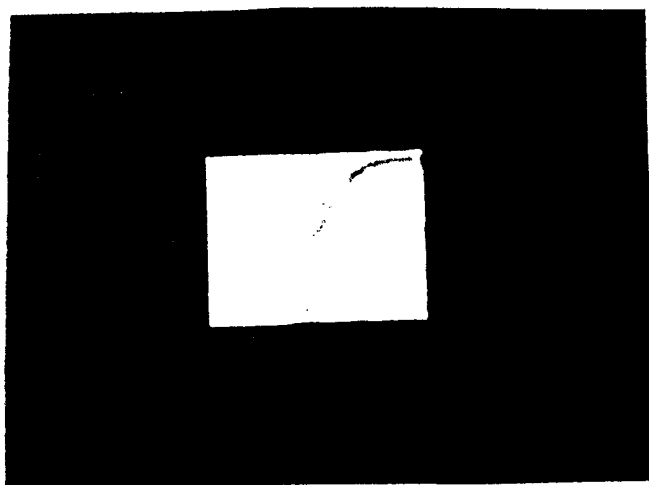
(c)



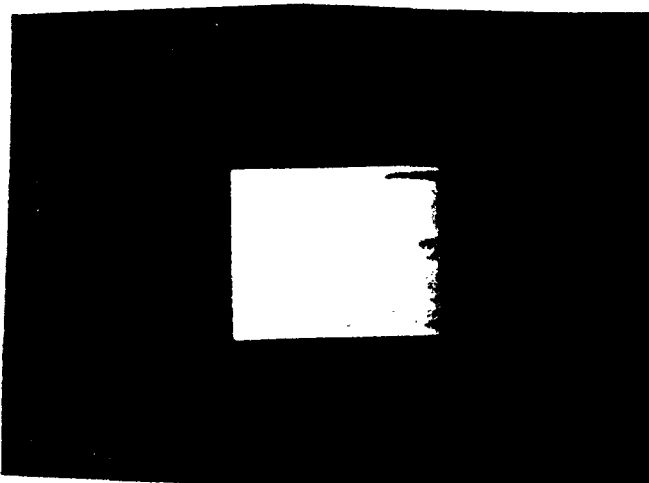
(d)



(e)



(a)



(b)

Figure 11. Set of Images of a Dollar Bill

(a) The original image.

(b) The blurred image with  $d = 45$  and  $\theta = 0$ .

(c) The blurred image with  $d = 35$  and  $\theta = 45^\circ$ .

(d) The deblurred image obtained by implementing the reverse mapping algorithm on image (b).

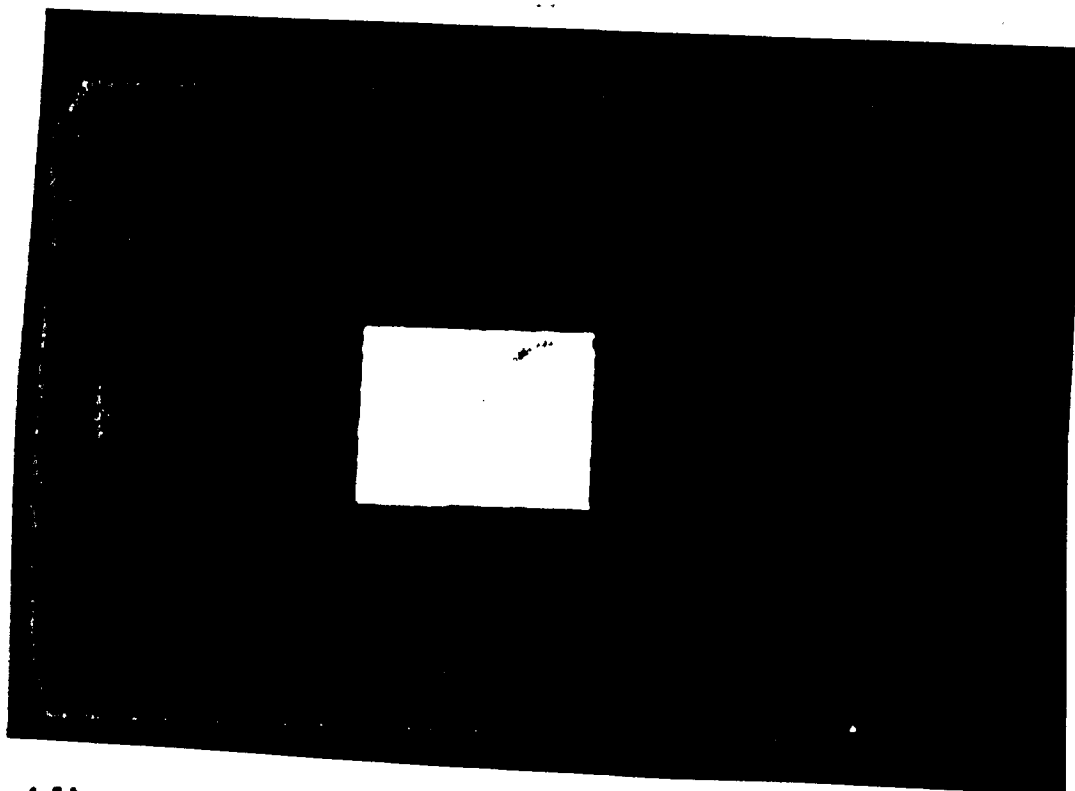
(e) The deblurred image obtained by implementing the reverse mapping algorithm on image (c).

Where  $d$  is blur parameter and  $\theta$  is the angle between the direction of motion and the  $x$  axis.

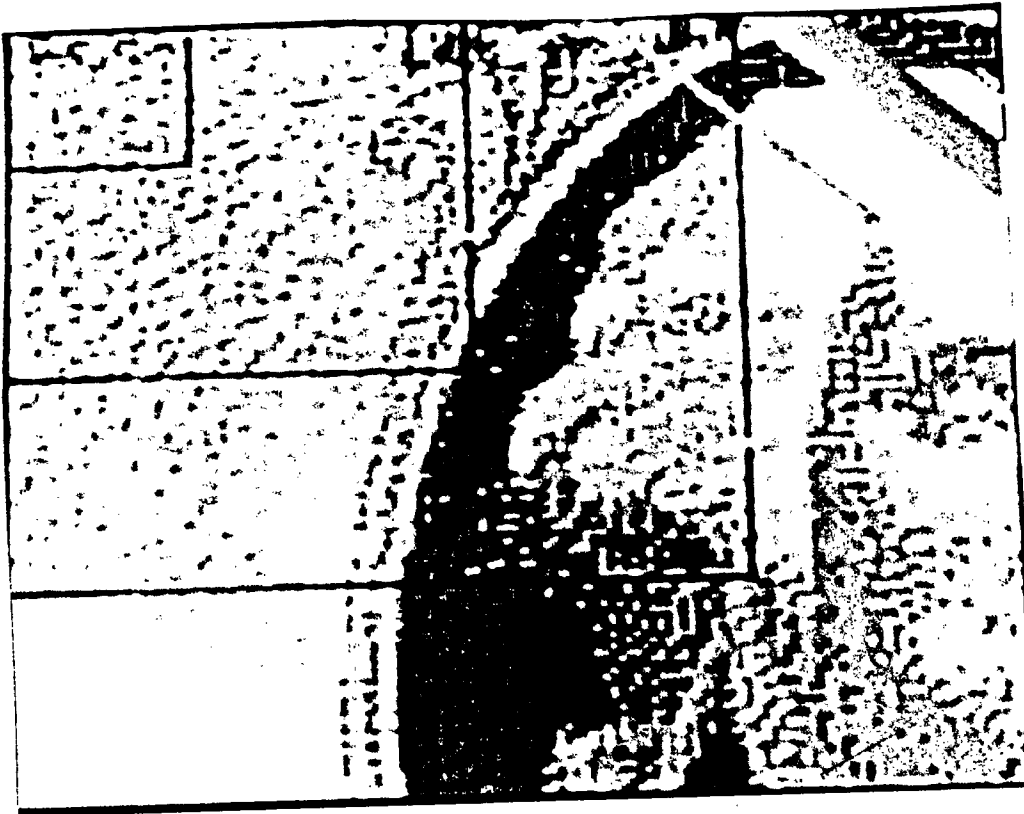




(c)



(d)



(e)

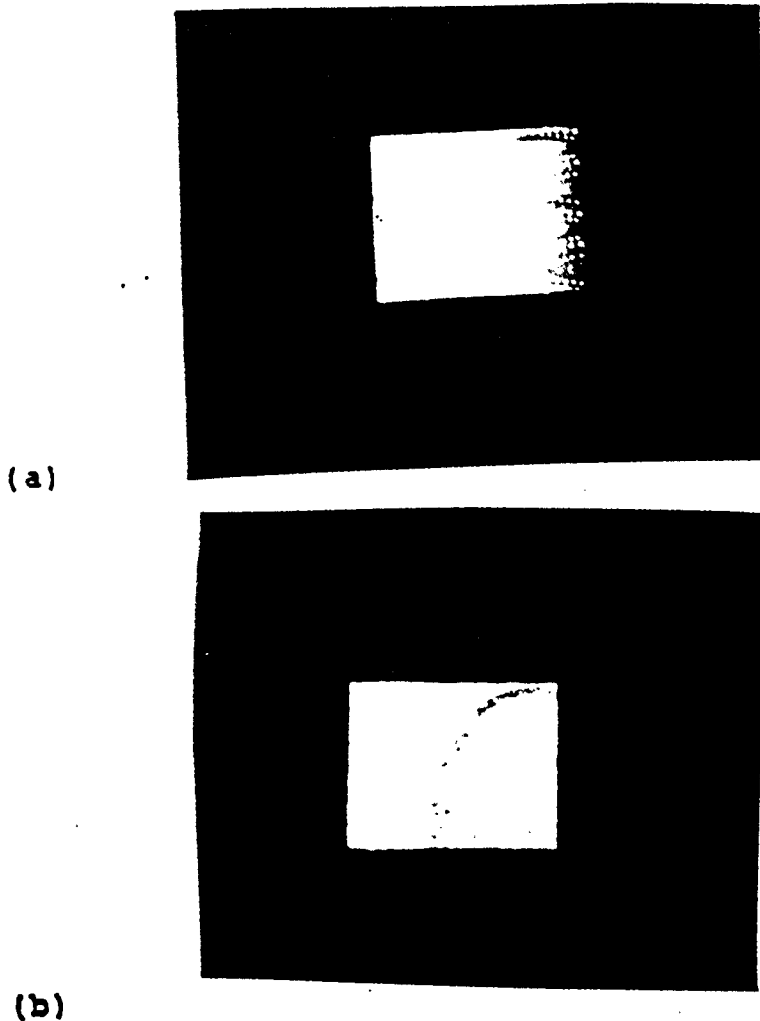
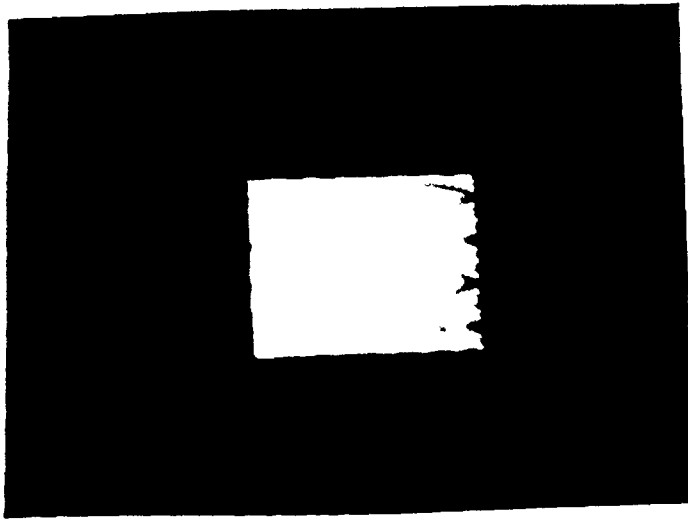


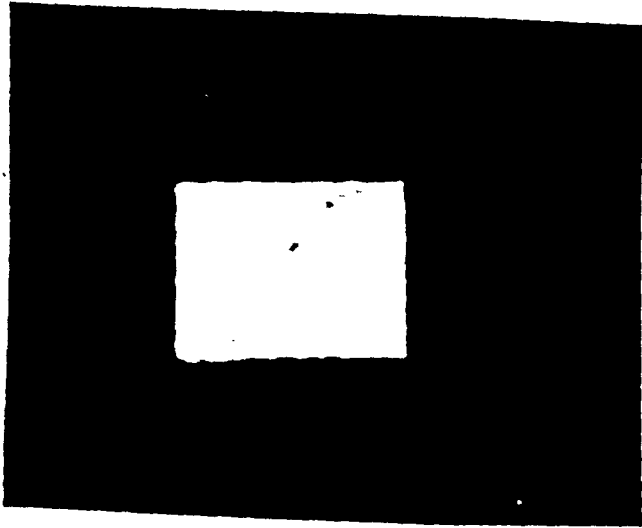
**Figure 12. Noise Performance on a Dollar Bill**

- (a) The blurred image with additive noise at  $SNR = 3.0$ .
- (b) The deblurred image obtained by implementing the reverse mapping algorithm on image (a).
- (c) The blurred image with additive noise at  $SNR = 1.0$ .
- (d) The deblurred image obtained by implementing the reverse mapping algorithm on image (c).
- (e) The blurred image with additive noise at  $SNR = 0.25$ .
- (f) The deblurred image obtained by implementing the reverse mapping algorithm on image (e).

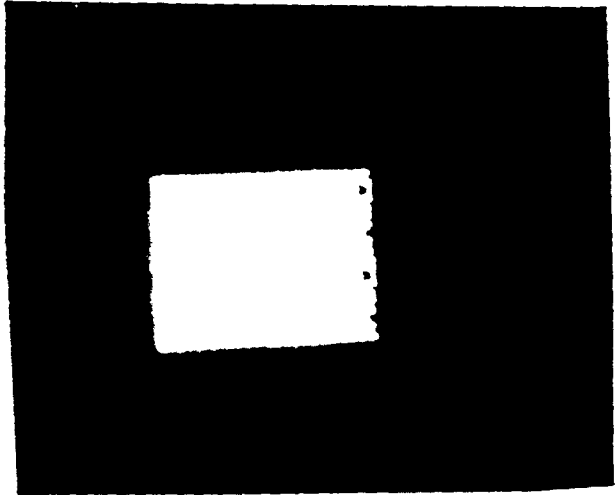
For all the blurred images the value of the blur parameter is 35 and the motion is along the x direction. The original image is an image of a dollar bill.



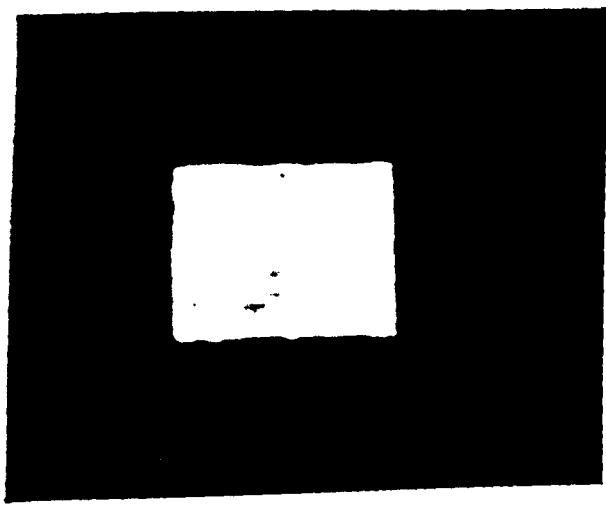
(c)



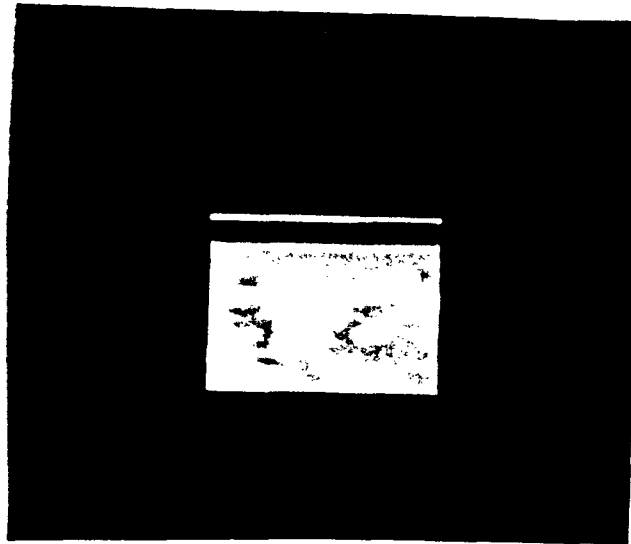
(d)



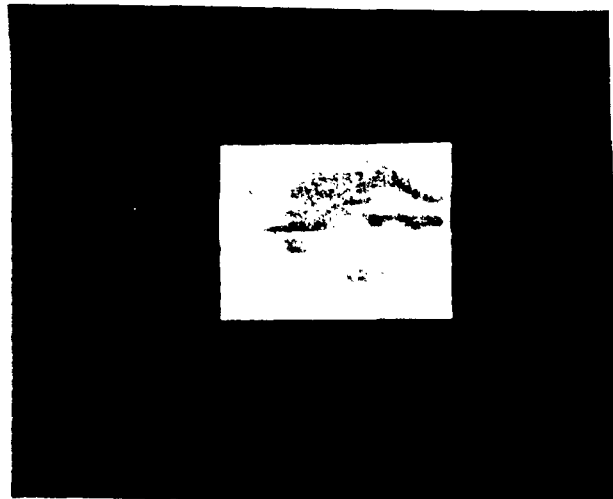
(e)



(f)



(a).



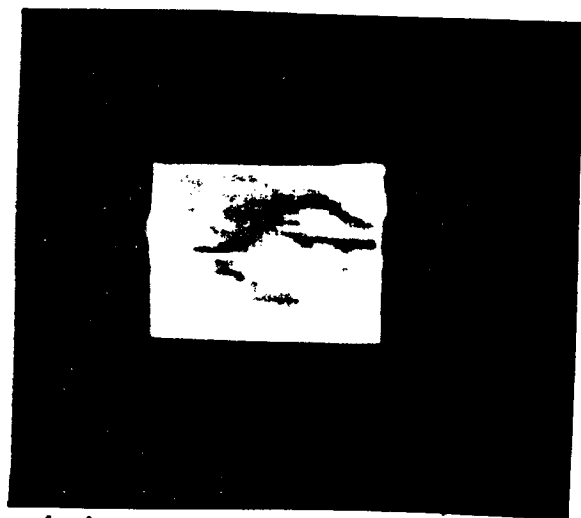
(b)

**Figure 13. Robber's Images**

(a) The original robbers image after magnification.

(b) The deblurred robbers image.

(c) The image obtained by equalizing the histogram of image (b).



(c)

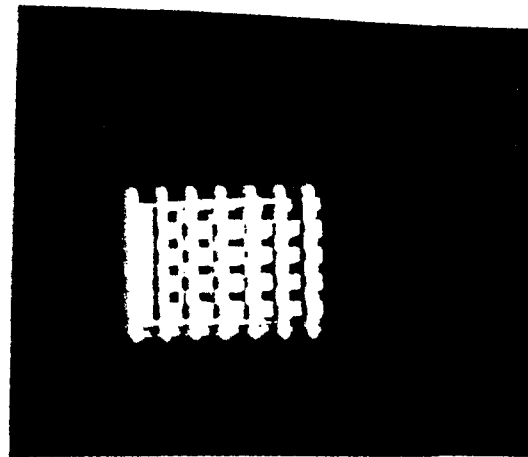
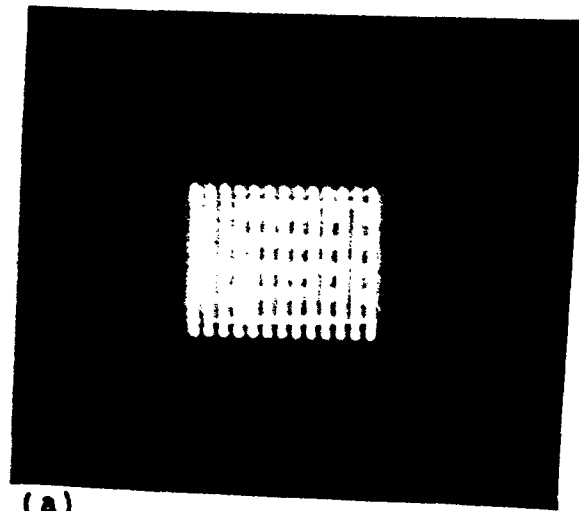
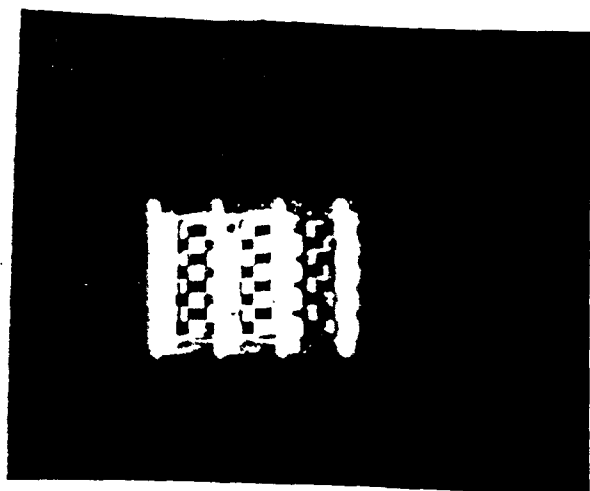


**Figure 14. Blur Parameter Sensitivity**

- (a) Deblurred image of the chessboard with blur parameter  $d = 10$  and actual blur parameter = 30.
- (b) Deblurred image of the chessboard with blur parameter  $d = 20$  and actual blur parameter = 30.
- (c) Deblurred image of the chessboard with blur parameter  $d = 40$  and actual blur parameter = 30.

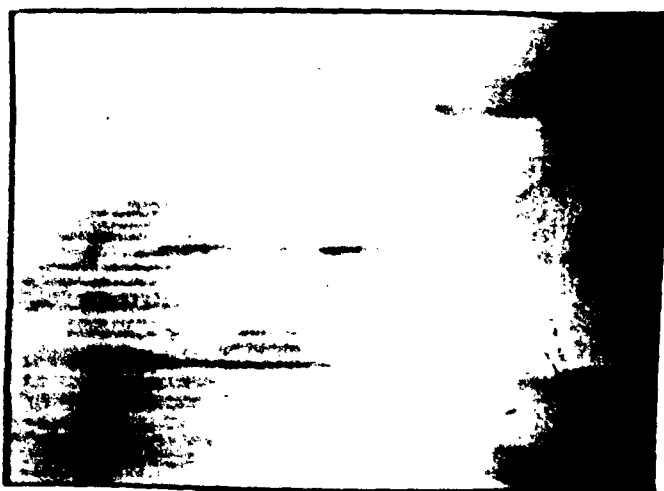




(c)



(a)



(b)

**Figure 15. Set of Images of the face of a lady**

(a) The original image.

(b) The blurred image with  $d = 40$  and  $\theta = 0$ .

(c) The deblurred image obtained by implementing the reverse mapping algorithm on image (b).



(c)

## CHAPTER IV

### SUMMARY AND CONCLUSIONS

This thesis addresses the problem of restoring images blurred by linear and spatially invariant rigid body motion blurs.

The first chapter defines the problem of restoring images blurred by linear and spatially invariant rigid body motion blur. The sources and types of motion blurs are discussed in brief. The impulse responses of these motion blurs are studied. A brief study of cepstrum domain is done in context to image restoration. A brief survey of image restoration techniques and their applications is done.

An analysis of three image restoration techniques is done in the second chapter. These three image restoration techniques include the dynamical model implementation (state-space approach) by Silverman et al. [11] - [13], Sondhi's [2] method of using the background pixels and the Landweber's iteration by Trussell et al. [14]-[18]. The results of these three image restoration techniques, used to develop the reverse mapping algorithm, are established. Some image restoration techniques of historical significance are introduced. All image restoration techniques need an accurate estimate of the blur parameter. A brief study of

data extraction techniques is done in three domains, namely, the spatial domain, the frequency domain and the cepstrum domain. A model proposed by Cannon [31] to estimate the blur parameter in the cepstrum domain is briefly discussed. In the later part of the second chapter two models for multiple motion blurs are presented, namely, the double convolution model and the bilinear model.

In the third chapter a new algorithm for restoration of motion blurs is presented in detail. This algorithm involves spatial domain iterative restoration of motion blurs. The algorithm is implemented on images blurred by linear and spatially invariant rigid body motion blur. The results are provided in the later part of the third chapter. The algorithm is then extended to a general degradation. The implementation issues of this algorithm are tackled in the later part of the third chapter.

The robustness of the algorithm proposed in the third chapter can be seen from the results. The algorithm has a good performance in deblurring motion blurred images with the loss of information coefficient as high as 50%. The algorithm preserves the blur model intact during deblurring. This provides a strong control over the generated noise. The algorithm has a good performance in deblurring motion blurred images, corrupted with additive noise having a signal-to-noise ratio as low as 1.00. This performance

establishes the ability of the algorithm to pick up noisy pixels.

The algorithm is computationally simpler as compared to other spatial domain image restoration techniques. The algorithm operates on sets of periodic numbers, with a period equal to the blur parameter  $d$ . Thus the number of calculations are reduced from the order of the original signal  $M$ , to the blur parameter  $d$ .

This algorithm is highly successful in deblurring motion blurs and hence is very reliable. The reliability of this algorithm could be used to find the value of the blur parameter. The algorithm is also independent of the blur model. The algorithm could therefore be implemented on other types of motion blurs, focus blurs or multiple blurs.

## APPENDIX A

Impulse responses of different types of blurs are given below. In all the equations  $(x,y)$  and  $(u,v)$  denote the spatial coordinates and the frequency coordinates respectively.  $\delta(\theta)$  stands for an unit impulse in a direction making an angle  $\theta$  with x axis. T is the total time for which the object is in motion. Sondhi [2] has proved the following results in detail.

### A.1 Uniform Linear Motion in a Direction $\delta(\theta)$

Linear motion is in a random direction  $\delta(\theta)$  with a variable velocity  $V(\theta,t)$ .  $\delta(\theta')$  is perpendicular to  $\delta(\theta)$ .

$$\begin{aligned} h(x,y) &= \delta(\theta') (1/V(\theta,t)) \quad \text{for } 0 \leq x \leq d \cos(\theta) \\ & \qquad \qquad \qquad \qquad \qquad \qquad 0 \leq y \leq d \sin(\theta) \\ &= 0 \qquad \qquad \qquad \qquad \qquad \qquad \text{else } \dots \dots \dots ( A-1a ) \end{aligned}$$

If  $V(\theta,t)$  is constant, the motion becomes an uniform linear motion. The frequency response is as follows.

$$\begin{aligned} H(u,v) &= \sin (\pi d f) / (\pi d f) \\ &= \text{sinc} (\pi d f) \qquad \dots \dots \dots ( A-1b ) \end{aligned}$$

Where

$$f = u \cos(\theta) + v \sin(\theta)$$

### A.2 Uniform Linear Motion in the x Direction

This is a special case of uniform linear motion. The impulse response is obtained by putting  $\theta = 0$  in Equation ( A-1a ) and Equation ( A-1b ).

$$\begin{aligned} h(x,y) &= 1/d \quad \text{for } y = 0 \text{ and } 0 \leq x \leq d \\ &= 0 \quad \text{else} \\ H(u,v) &= \text{Sinc} (\pi du) \quad \dots\dots\dots ( A-2 ) \end{aligned}$$

### A.3 Rotational Blur around Infinite Axes

In this type of blur all the axes are parallel to each other. This blur involves a rigid object. The velocity at any instant  $t$  is then given by its two components  $V_x(t)$  and  $V_y(t)$ .

$$\begin{aligned} V_x(t) &= d \text{ Cos} (2\pi at/T) \\ V_y(t) &= d \text{ Sin} (2\pi at/T) \quad \dots\dots\dots ( A-3a ) \end{aligned}$$

Where

$a$  : is a constant denoting the arc moved.

$T$  : the total time in motion.

The frequency response is as follows.

$$H(u,v) = J_0 ( 2\pi d \sqrt{(u^2+v^2)} ) \quad \dots\dots\dots ( A-3b )$$

Where

$J_0$  : is the zeroth order Bessel's function.



#### A.4 Rotational Blur around One Axis

Rotational blur about a constant axis has a spatially variant PSF in the cartesian coordinates. Let the constant angular velocity be  $\Omega$ . Then Equation ( A-4 ) gives the degraded image as a function of the original image.

$$g(x,y) = \frac{\int_C f( x-r\cos(\Omega l) , y+r\sin(\Omega l) ) dl}{\int_C dl} \dots\dots\dots ( A-4 )$$

Where

$$r : \sqrt{(x^2+y^2)}$$

$$\Omega l = \text{Tan}^{-1}(y/x) + l/r$$

C : is a arc of the circle with center (0,0) and radius r from angle 0 to  $\Omega T$ .

#### A.5 Spatially Invariant Focus Blur

The impulse response for spatially invariant focus blur is given by Equation ( A-5 ).

$$\begin{aligned} h(x,y) &= 1/(\pi R^2) && \text{for } r \leq R \\ &= 0 && \text{else} \end{aligned}$$

$$H(u,v) = J_1(Rr) / (Rr) \dots\dots\dots ( A-5 )$$

where

J<sub>1</sub> : is the first order Bessel's function.

R : is the defocus radius.

$$r : \sqrt{(x^2+y^2)}.$$

### A.6 Z directional motion.

It is a blur caused by motion of the object parallel to camera axis. This produces a focus blur.

$$\begin{aligned}
 h(x,y) &= (1/K) [(L1-z)d1 + (L2-z)d2] \quad \text{for } r \leq R \\
 &= 0 \quad \text{else} \\
 &\dots\dots\dots ( A-6 )
 \end{aligned}$$

where

R : is the maximum defocus radius attained during the motion.

$$r : \sqrt{(x^2+y^2)}$$

L1 : is the maximum distance reached in the positive z direction.

L2 : is the maximum distance reached in the negative z direction.

U : the unit step function.

$$d1 : U(z) - U(L1-z)$$

$$d2 : U(z) - U(L2-z)$$

## APPENDIX B

The properties of convex sets are established for the weighted means and the mean square error bounds.

Let  $x_1$  and  $x_2$  be two members of a closed convex set  $\Phi$  with pixel limit 0 and 255. If  $x_3$  is a weighted average of  $x_1$  and  $x_2$  then  $x_3$  is also a member of  $\Phi$ . Hence  $x_3$  follows all the mathematical properties of the convex set  $\Phi$ . The proof of this statement for the weighted mean and the mean squared error bounds is given in the following sections.

Given that if  $x_1$  and  $x_2 \in \Phi$

and  $x_3 = \alpha x_1 + (1-\alpha) x_2$  for  $0 \leq \alpha \leq 1$

then  $x_3 \in \Phi$ .

### B.1 Weighted Mean

If  $0 \leq x_1 \leq 255$  and  $0 \leq x_2 \leq 255$ ,

then

$0 + (1-\alpha) 0 \leq \alpha x_1 + (1-\alpha) x_2 \leq 255 (\alpha + 1 - \alpha)$

$\Rightarrow 0 \leq x_3 \leq 255$

### B.2 Mean Squared Error bounds

If  $\|g - hx_1\|^2 \leq \delta v$

$\|g - hx_2\|^2 \leq \delta v$

where  $\delta v$  : is the mean square error bound.

then

$$\begin{aligned}
 ||g - hx_3||^2 &= ||g - h(ax_1 + (1-a)x_2)||^2 \\
 \Rightarrow ||g - hx_3||^2 &= ||a(g - hx_1) + (1-a)(g - hx_2)||^2 \\
 &= a^2 ||g - hx_1||^2 \\
 &\quad + 2a(1-a) ||g - hx_1|| ||g - hx_2|| \\
 &\quad + (1-a)^2 ||g - hx_2||^2 \\
 \Rightarrow ||g - hx_3||^2 &\leq \delta v (a^2 + 2a(1-a) + (1-a)^2) \\
 \Rightarrow ||g - hx_3||^2 &\leq \delta v
 \end{aligned}$$

APPENDIX C

The residual during an iterative spatial domain technique is given by Equation ( C-1 ).

$$r = g - h f^m \dots\dots\dots ( C-1 )$$

Where

$f^m$  : is the estimate after  $m^{th}$  iteration.

$r$  : is the residual after  $m^{th}$  iteration.

$g$  : is the degraded image.

$h$  : is the impulse response.

The constraint is then placed on this residual signal  $r$ . This often forms the criteria of exit from the iteration. If this constraint placed is  $r = 0$ , then there would be no solution in the real domain in the presence of noise. Sondhi [2] and Trussell et al. [18] suggested the use of noise statistics as a solution to this problem. This method is given below.

Let the standard deviation of noise be  $\sigma$ . Then the criterion of exit from the iteration is as follows.

$$|| r ||^2 \leq || \sigma ||^2 \dots\dots\dots ( C-2 )$$

where

$r$  : is the residual given by equation ( C-1 ).

$\sigma$  : is the standard deviation of noise.

Equation ( C-2 ) is not the definition of feasible set.

Trussell et al. [14] and [16] investigated these definitions in detail. These are different since feasible set has other constraints imposed on it, in addition to the constraint given by Equation ( C-2 ). Feasible set is an intersection of all the constraints including the one given by Equation ( C-2 ).

APPENDIX D

Singular impulse matrix makes it necessary to take precautions against the null vectors. This problem is illustrated below.

Let  $\mu$  be a null eigenvector of the impulse matrix. It could be associated with any one of the zero eigenvalues of this matrix. Equation ( D-1 ) proves that the contribution of any scalar multiple of this vector to the iteration is zero. This proves that there are infinite solutions to any degraded image if the impulse matrix is singular ( has at least one zero eigenvalue ). The matrix notations are neglected for convenience.

Since  $\mu$  is a null eigenvector

$$h \mu = 0$$

therefore,

$$\begin{aligned} h (f^{\phi+1} + k\mu) &= h f^{\phi} + k h \mu \\ &= h f^{\phi} \end{aligned} \quad \text{..... ( D-1 )}$$

where

$f^{\phi}$  : is the estimate after  $\phi^{\text{th}}$  iteration.

$h$  : is the impulse response.

This has to be taken into account before deciding the step size for an iteration. The step size should not be a scalar multiple of the null eigenvector.

In the algorithm described in Chapter three, the eigenvalues of the nonsingular part of the impulse matrix  $[h]$  decides the rate of convergence of the iteration.  $M - N$  zero eigenvalues get discarded by defining the non singular part of the impulse matrix. Trussell et al. [14] proved that these remaining eigenvalues are important in deciding the constraints control implementation - " Small but non zero eigenvalues were shown to be the cause slow rate of convergence in the class of iterative signal restoration methods ".



APPENDIX E

The continuity constraints are implemented by imposing bounds on the derivatives of the pixels.

Let  $\delta^1, \delta^2, \dots, \delta^n$  be arbitrary positive numbers. Then these constraints are implemented as in Equation ( E-1 ).

$$\begin{aligned} |g'(x,y)| , |f'(x,y)| &\leq \delta^1 \\ |g''(x,y)| , |f''(x,y)| &\leq \delta^2 \\ \cdot &\quad \cdot \quad \cdot \quad \cdot \\ |g^n(x,y)| , |f^n(x,y)| &\leq \delta^n \quad \dots\dots\dots ( E-1 ) \end{aligned}$$

where

' , '' , ... , <sup>n</sup> give the order of the derivative.

It is apparent that even the signal bound is a constraint on a derivative of order 0.

APPENDIX F

Trussell et al. [14] used the landweber's iteration for restoration of blurred images. Landweber's iteration is as follows.

$$f^{m+1} = f^m + L h^t (g - h f^m) \dots\dots\dots ( F-1 )$$

where

- m : is the order of iteration.
- h : is the impulse matrix ( t for transpose ).
- L : is a matrix which can modify the convergence properties but not the solution.

This iteration has a guaranteed convergence. For L = I, and some random initial estimate f<sup>0</sup>, the estimates of the original signal f are given Equation ( F-2 ). The matrix notations are neglected for convenience.

$$f^1 = (1 - h^t h) f^0 + h^t g$$

$$f^2 = (1 - h^t h) f^1 + h^t g$$

thus,

$$f^n = r^n f^0 + \left( \sum_{i=0}^{n-1} r^i h^t \right) g \dots\dots\dots ( F-2 )$$

where

$$r = 1 - h^t h.$$

The summation is a geometric series with known

convergence properties. Trussell et al. [14] proved that this value will converge to  $\Omega$  ( if  $\Gamma \leq 1$  ).

Where  $\Omega = X + C f^\infty$

Then any row  $p$  of  $F$  is given as follows.

$$\begin{aligned}
 C_p &= 0 && \text{if } h_p^t h = 0 \\
 &= I_p && \text{if } h_p^t h \neq 0 \\
 X_p &= f_p^0 && \text{if } h_p^t h = 0 \\
 &= 0 && \text{if } h_p^t h \neq 0 \\
 \Omega_p &= f_p^0 && \text{if } h_p^t h = 0 \\
 &= f_p^\infty && \text{if } h_p^t h \neq 0
 \end{aligned}$$

..... ( F-3 )

## APPENDIX G

The conditional expectation used in the algorithm in Chapter three is a noise shield. This function checks whether the pixel is noisy.

Let  $\delta_n$  be a bound on the derivative of the signal and let  $\sigma$  be the standard deviation of noise. Then a pixel can be defined as noisy, if Equation ( G-1 ) is true.

$$| g'(x,y) | \leq \delta + \sigma \quad \dots\dots\dots ( G-1 )$$

where

$g'(x,y)$  : is the first order derivative of the degraded signal.

$\delta$  : is the maximum bound on the derivative.

$\sigma$  : is the standard deviation of noise.

## Bibliography

1. D.H.Ballard and C.M.Brown, Computer Vision. Prentice-Hall, Englewood Cliffs, New Jersey, USA 1982.
2. M.M.Sondhi, "Image restoration: The removal of spatially invariant degradations," Proc. of IEEE, vol.60, No.7, July 1972, pp. 842-853.
3. J.L.Harris Sr., "Image evaluation and restoration," Journal Optical Society of America, vol.56, May 1966, pp. 569-574.
4. J.L.Harris Sr., "Potential and limitations of techniques for processing linear motion degraded imagery," Evaluation of motion degraded images, Washington D.C: U.S. Government Printing Office, 1968, pp. 131-138.
5. J.L.Horner, "Optical spatial filtering with least mean square error filter," Journal Optical Society of America, vol.59, May 1969, pp. 553-558.
6. J.L.Horner, "Optical restoration of images blurred by atmospheric turbulence using optimum filter theory," Applied Optics, vol.9, January 1970, pp. 167-171.
7. C.W.Helstrom, "Image restoration by the method of least squares," Journal of Optical Society of America, vol.57, March 1967, pp. 297-303.
8. D.Slepian, "Linear least square filtering of distorted images," Journal of Optical Society of America, vol.57, July 1967, pp. 918-922.

9. D.Slepian, "Restoration of photographs blurred by image motion," *Bell Systems Technical Journal*, vol.46, Dec. 1967, pp. 2353-2362.
10. D.P.McAdam, "Digital image restoration by constrained deconvolution," *Journal of Optical Society of America*, vol.60, December 1970, pp. 1617-1627.
11. A.O.Aboutalib, M.S.Murphy and L.M.Silverman, "Digital restoration of images degraded by general motion blurs," *IEEE trans. on Automatic Control*, vol. AC-22, No 3, June 1977, pp. 294-302.
12. L.M.Silverman, "Realization of linear dynamical systems," *IEEE trans. on Automatic Control*, vol. AC-16, Dec. 1971, pp. 554-567.
13. A.O.Aboutalib and L.M.Silverman, "Restoration of motion degraded images," *IEEE trans. on Circuits Systems*, vol. CAS-22, March 1975, pp. 278-286.
14. H.J.Trussell and M.R.Civanlar, "The feasible solution in signal restoration," *IEEE trans. on Acoustics, Speech and Signal Processing*, vol. ASSP-32, No.2, April 1984, pp. 201-211.
15. H.J.Trussell and M.R.Civanlar, "The initial estimate in constrained iterative restoration," *Proc of IEEE International Conf. Acoustics, Speech and Signal Processing*, April 1983.
16. H.J.Trussell, "A priori knowledge in algebraic restoration methods," *Advanced Computer Vision and Image Processing*, vol.1, 1984.

17. B.R.Hunt, "The application of constrained least squares estimation to image reconstruction by digital computer," IEEE trans. on Computers, vol. C-32, Sept. 1973, pp. 805-812.
18. H.J.Trussell, "Convergence criteria for iterative restoration methods," IEEE trans. on Acoustics, Speech and Signal Processing, vol. ASSP-31, No.1, Feb. 1983, pp. 129-136.
19. D.E.Dudgeon, "An iterative implementation of 2-D digital filter," IEEE trans. on Acoustics, Speech and Signal Processing, vol. ASSP-28, December 1980, pp. 666-671.
20. R.M.Leahy and C.E.Goutis, "An optimal technique for constraint-based image restoration and reconstruction," IEEE trans. on Acoustics, Speech and Signal Processing, vol. ASSP-34, No.6, December 1986, pp. 1629-1642.
21. Y.S.Shim and Z.H.Cho, "SVD pseudoinversion image restoration," IEEE trans. on Acoustics, Speech and Signal Processing, vol. ASSP-29, No.4, August 1981, pp. 904-909.
22. D.G.Childers, D.P.Skinner and R.C.Kemerkait, "The cepstrum: A guide to processing," Proc of IEEE, vol.65, No.10, October 1977, pp. 1428-1443.
23. H.M.Kim and N.K.Bose, "Approaches towards restoration of bilinearly degraded images," IEEE trans. on Acoustics, Speech and Signal Processing, vol.ASSP-35, No.2, February 1987, pp. 181-197.

24. T.J.Broida and R.Chellapa," Estimation of object parameters from noisy images," IEEE trans. on Pattern Analysis and Machine Intelligence, vol.PAMI-8, No.1, January 1986, pp. 90-98.
25. A.M.Tekalp, H.Kaufman and J.W.Woods,"Identification of image and blur parameters for the restoration of noncausal blurs," IEEE trans. on Acoustics,Speech and Signal Processing, vol. ASSP-34, No.4, August 1986, pp. 963-971.
26. E.Oja and H.Ogawa," Parametric projection filter for image and signal restoration," IEEE trans. on Acoustics, Speech and Signal Processing, vol. ASSP-34, No.6, December 1986, pp. 1643-1653.
27. M.Ahmadi and R.A.King, " A stability criterion for N-dimensional zero-phase recursive digital filters," Proc of IEEE, vol.65, June 1977, pp. 893-898.
28. A.Z.Meiri,"On monocular perception of 3-D moving objects ," IEEE trans. on Pattern Analysis and Machine Intelligence, vol.PAMI-2, No.6, November 1980, pp. 582-583.
29. A.V.Oppenheim, G.E.Kopec and J.M.Tribolet," Signal analysis by homomorphic prediction," IEEE trans. on Acoustics, Speech and Signal Processing, August 1976, pp. 329-332.
31. M.Cannon," Blind deconvolution of spatially invariant image blurs with phase," IEEE trans. on Acoustics,



- Speech and Signal Processing, vol. ASSP-24, No.1, February 1976, pp. 58-63.
32. M.Soumekh," Image reconstruction techniques in tomographic imaging systems," IEEE trans. on Acoustics, Speech and Signal Processing, vol. ASSP-34, No.4, August 1986, pp. 952-962.
  33. X.Zhuang, E.Ostevold and R.M.Haralick,"A differential approach to maximum entropy image reconstruction," IEEE trans. on Acoustics, Speech and Signal Processing, vol. ASSP-35, No.2, February 1987, pp. 208-218.
  34. H.C.Andrews and B.R.Hunt, Digital Image Restoration. Englewood Cliffs, New Jersey, Prentice-Hall, 1977, pp. 152-154.
  35. A.V.Oppenheim and R.W.Schafer, Digital Signal Processing. Prentice-Hall, Englewood Cliffs, New Jersey, USA, 1975.
  36. A.Rosenfeld and A.C.Kak, Digital Picture Processing. 2nd Ed. vol. 1, New York:Academic, 1982.
  37. A.M.Tekalp and H.J.Trussell,"Comparative study of some recent statistical and set-theoretic methods for image restoration," Proceedings of 1988 IEEE International Conference on ASSP, pp. 988-991.
  38. A.M.Tekalp, H.Kaufman and J.W.Woods,"Decision-directed segmentation for the restoration of images degraded by a class of space-variant blurs," Proceedings of 1988 IEEE International Conference on ASSP, pp. 980-983.

39. D.Angwin, H.Kaufman,"Image restoration using a reduced order model Kalman filter," Proceedings of 1988 IEEE International Conference on ASSP, pp. 1000-1003.

VITA AUCTORIS

- 1965 Born May 5th, Ottawa, Ontario, CANADA.
- 1982 Higher Secondary  
S.I.E.S College, Sion, Bombay, INDIA.
- 1986 B.Tech. Electrical Engineering  
Indian Institute of Technology, Bombay, INDIA.
- 1989 Master of Applied Science Electrical Engineering  
University of Windsor, Windsor, Ontario, CANADA.